LU TP 13-38
USM-TH-322
May 2014

Higgsstrahlung at forward rapidities

Roman Pasechnik*

Department of Astronomy and Theoretical Physics,
Lund University, SE 223-62 Lund, Sweden

B.Z. Kopeliovich and I.K. Potashnikova

Departamento de Física, Universidad Técnica Federico Santa María; and
Centro Científico-Tecnológico de Valparaíso,
Avda. España 1680, Valparaíso, Chile

Abstract

We discuss the inclusive and single diffractive heavy flavor (top and bottom) production in association with the Higgs boson at forward rapidities in proton-proton collisions at the LHC. The calculations are performed in the framework of the phenomenological dipole approach, which automatically accounts for the absorptive corrections induced by soft interactions, i.e. for the gap survival effects at the amplitude level. Major differential observables including the realistic ATLAS detector constraints are considered. The forward inclusive and diffractive Higgsstrahlung processes are generated essentially by excitation of the valence or sea quarks in the proton. The single diffractive Higgsstrahlung off top quarks is found to dominate compared to the loop-induced mechanism at sufficiently large Higgs boson transverse momenta. The Higgsstrahlung processes offer a direct and precise measurement of Higgs-top and, possibly, Higgs-bottom Yukawa couplings at the LHC, as well as the studies of the intrinsic heavy flavor components of the proton.

PACS numbers: 13.87.Ce, 14.65.Dw, 14.80.Bn

*Electronic address: Roman.Pasechnik@thep.lu.se

I. INTRODUCTION

The Higgs boson recently discovered at the LHC [1, 2] appears to be one of the most prominent standard candles for the physics within and beyond the Standard Model (SM) (for more details of the Higgs physics highlights at the LHC see e.g. reviews [3, 4] and references therein). Most of the SM extensions predict stronger or weaker distortions in Higgs boson Yukawa couplings. In this sense, measurements of the Higgs-heavy quarks couplings becomes a very important task of the ongoing Higgs physics studies at the LHC and serves as one of the major probes for the signals of New Physics.

Phenomenological tests of a number of New Physics scenarios at a TeV energy scale relies upon our understanding of the underlined QCD dynamics and backgrounds. The QCD-initiated gluon-gluon fusion mechanism is one of the dominant Higgs bosons production modes in inclusive pp scattering which has contributed to its discovery at the LHC [1, 2]. The hard loop induced amplitude has been studied in a wealth of theoretical articles so far. The inclusive cross section has been calculated at up to next-to-next-to-leading order in QCD [5–10]. Also, the QCD soft-gluon re-summation at up to next-to-next-to-leading logarithm approximation was performed in Ref. [11] and the next-to-leading order factorized electroweak corrections were incorporated in Ref. [12]. Besides the standard collinear factorisation approach, the inclusive Higgs boson production has been studied in the $k_\perp$-factorisation framework in Refs. [13, 14]. The inclusive associated production of the Higgs boson and heavy quarks has been thoroughly analyzed in the $k_\perp$-factorisation in Ref. [15].

The studies of inclusive Higgs boson production typically suffer from large Standard Model backgrounds and theoretical uncertainties, strongly limiting this channel's potential for tracking small New Physics effects. As a promising way out, the exclusive and diffractive Higgs production processes offer new possibilities to constrain the backgrounds, and open up more opportunities for New Physics searches (see e.g. Refs. [16–19]). Likewise in inclusive production, the loop-induced gluon-gluon fusion $gg \to h$ mechanism is expected to be an important Higgs production channel in single diffractive pp scattering as well, while this is the only possible mechanism for the central exclusive Higgs production [16].

Once the poorly known nonperturbative elements are constrained by pure SM-driven data sets, they can also be applied for description of other sets of data potentially sensitive to New Physics contributions. This way, it would be possible to pin down and to constrain the yet unknown sources of theoretical uncertainties purely *phenomenologically* to a precision sufficient for searches of new phenomena at the LHC.

In particular, diffractive production of heavy flavored particles at forward rapidities is often considered as one of the important probes for the QCD dynamics at large distances, which can be efficiently constrained by data. Within the color dipole approach [20] a diffractive process looks like elastic scattering of $\bar{q}q$ dipoles of different sizes, and of higher Fock states containing more partons. In particular, it provides a prominent way to study the diffractive factorisation breaking effects due to an interplay between hard and soft interactions. Previously, the latter effects have been successfully studied in the case of forward Abelian radiation of virtual photons (diffractive Drell-Yan reaction) in Refs. [21, 22], as well as for the more general case of forward gauge bosons production [23], and in the non-Abelian case of the forward heavy flavor production [24].

Based on the formalism developed earlier [23, 24], we employ the color dipole approach specifically for the inclusive and single diffractive Higgs boson production in association with

a heavy quark pair in proton-proton collisions at the energies of LHC. Since the universal dipole cross section, entering the inelastic amplitudes squared and the diffractive amplitudes, is well constrained by the phenomenology at both large [25] and small [26] transverse dipole separations, one would expect that the typically large QCD uncertainties in the cross sections of diffractive Higgs boson production to be significantly reduced. Potentially, this should allow precise studies of the Higgs boson Yukawa couplings to heavy quarks.

Since Higgs boson-quark couplings in the SM are proportional to the quark masses, a significant contribution to the Higgs production at forward rapidities comes from the Higgsstrahlung process off heavy quarks (predominantly, off bottom b and top t quarks) in the proton sea. Furthermore, in this work we do not take into consideration the Higgsstrahlung mechanism off the intrinsic heavy flavors, which was previously studied in Refs. [27, 28]. Here we consider diffractive Higgsstrahlung of heavy quarks produced via the perturbative gluon-gluon fusion mechanism. Meanwhile, the heavy quarks can emerge in the final state either as hadronic jets, or form a virtual loop. In the latter case one would not observe any other hard jets besides those coming from the hadronic Higgs decays (e.g. into $b\bar{b}$) with invariant mass distribution naturally peaking at the Higgs boson mass. We compare both cases and make conclusions about their relevance in both inclusive and single diffractive cases below.

The paper is organized as follows. Section II is devoted to a thorough discussion of inclusive Higgsstrahlung off heavy quarks, where the corresponding amplitudes and cross sections are derived within the dipole picture. Section III contains discussion and analysis of the diffractive Higgsstrahlung. In Section IV we present the main numerical results for differential distributions comparing Higgsstrahlung and loop-induced components for the realistic constraints by a detector. Finally, conclusions are made in Section V.

II. INCLUSIVE HIGGSSTRAHLUNG OFF HEAVY QUARKS

The kinematic variables for the Higgsstrahlung process in the quark-proton scattering illustrated in Fig. 1 are defined as follows: $p_{1,2}$ are the 4-momenta of the projectile and final quarks, respectively; $k_{1,2}$ are the 4-momenta of the produced heavy quarks Q and $\bar{Q}$ ($Q = c, b, t$) with mass m_Q, respectively; p is the 4-momentum of the produced Higgs boson h. As usual, we introduce the following notations for the light-cone decomposition keeping only the dominant Sudakov components, i.e.

$$k_1 \simeq (1-\beta-\gamma)q' - (\kappa+\tau)\,, \qquad k_2 \simeq \beta q' + \kappa\,, \qquad p \simeq \gamma q' + \tau\,, \tag{2.1}$$

where γ is the Higgs momentum fraction it takes from the parent heavy (anti)quark, β is the heavy (anti)quark momentum fraction is takes from the parent gluon, $q' \equiv k_1 + k_2 + p$ is the momentum of the hard gluon, which splits into the $\bar{Q}Qh$ system in the color field of the target proton. Further, we introduce notations for relative transverse momenta: (i) $\vec{\pi}$, between the final quark and the produced $\bar{Q}Qh$ system; (ii) $\vec{\kappa}$, between the Qh (or $\bar{Q}h$) pair and the heavy antiquark $\bar{Q}$ (or quark Q); and (iii) $\vec{\tau}$, between the Higgs boson and the parent gluon. They can be represented as,

$$\begin{aligned}
\vec{\pi} &= \alpha\vec{p}_2 - (1-\alpha)(\vec{k}_1 + \vec{k}_2 + \vec{p})\,,\\
\vec{\kappa} &= (1-\beta)\vec{k}_2 - \beta(\vec{k}_1 + \vec{p})\,,\\
\vec{\tau} &= (1-\gamma)\vec{p} - \gamma(\vec{k}_1 + \vec{k}_2)\,,
\end{aligned} \tag{2.2}$$

respectively, where α is the hard gluon momentum fraction is takes from the parent sea or valence quark in the projectile proton. It is useful to introduce Lorentz invariants,

$$Q^2 = -(p_1 - p_2)^2 > 0\,, \qquad M^2 = q'^2 > 0\,, \qquad M^2_{Qh}(k_{1,2}, p) = (k_{1,2} + p)^2 > 0\,. \tag{2.3}$$

They can be expressed in terms of the independent light-cone momenta

$$\begin{aligned} Q^2(\alpha, \vec{p}_2) &= \frac{\alpha^2 m_q^2 + \vec{p}_2^{\,2}}{1-\alpha}\,, \\ M^2(\beta, \vec{\kappa}; \xi, \vec{p}) &= \frac{(1-\beta)m_Q^2 + \beta M^2_{Qh}(\xi, \vec{p}) + \vec{\kappa}^{\,2}}{\beta(1-\beta)}\,, \\ M^2_{Qh}(\xi, \vec{p}) &= \frac{(1-\xi)M_h^2 + \xi m_Q^2 + \vec{p}^{\,2}}{\xi(1-\xi)}\,, \end{aligned} \tag{2.4}$$

where $\vec{p}_2 = \vec{\pi} + (1-\alpha)\vec{q}$ is the transverse momentum of the final valence quark q. The positive direction of the transverse momentum $\vec{q}$ of the t-channel gluon is chosen towards the target proton (see Fig. 2). Other new variables in Eq. (2.4),

$$\xi \equiv \frac{\gamma}{1-\beta}\,, \tag{2.5}$$

is the fractional light-cone momentum of the parent quark carried by the Higgs boson; and

$$\vec{p} \equiv \vec{\tau} + \frac{\gamma\,\vec{\kappa}}{1-\beta}\,, \tag{2.6}$$

is relative transverse momentum between the Higgs and parent (anti)quark. Thus, we introduced hereby the set of independent kinematical variables, α, $\vec{\pi}$; β, $\vec{\kappa}$; ξ, $\vec{p}$; $\vec{q}$, which will be used in what follows.

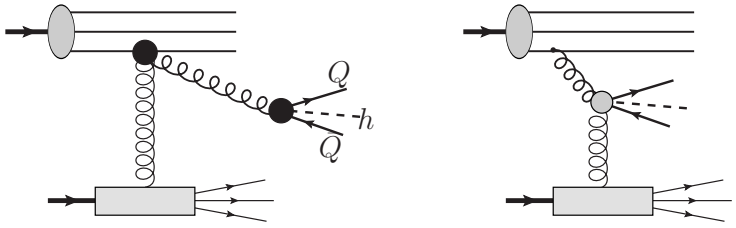

FIG. 1: Typical diagram topologies contributing to the inclusive $\bar{Q}Q + h$ production. Parton-level subprocesses denoted by filled large grey and bold circles are described separately in Fig. 2.

Further, defining the amplitudes, we will need to determine the kinematics transformation rules for the heavy quark and antiquark momenta being interchanged, i.e. for $k_1 \leftrightarrow k_2$. Under such a transformation we define a new set of variables expressed in terms of the old ones as follows,

$$\begin{aligned} \beta \;&\leftrightarrow\; \beta' \equiv (1-\xi)(1-\beta)\,, \qquad & \vec{\kappa} \leftrightarrow \vec{\kappa}\,' \equiv -\vec{p} - (1-\xi)\vec{\kappa}\,, \\ \xi \;&\leftrightarrow\; \xi' \equiv \frac{\xi(1-\beta)}{\beta + \xi(1-\beta)}\,, & \vec{p} \leftrightarrow \vec{p}\,' \equiv \frac{\beta\vec{p} - \xi\vec{\kappa}}{\beta + \xi(1-\beta)}\,, \end{aligned} \tag{2.7}$$

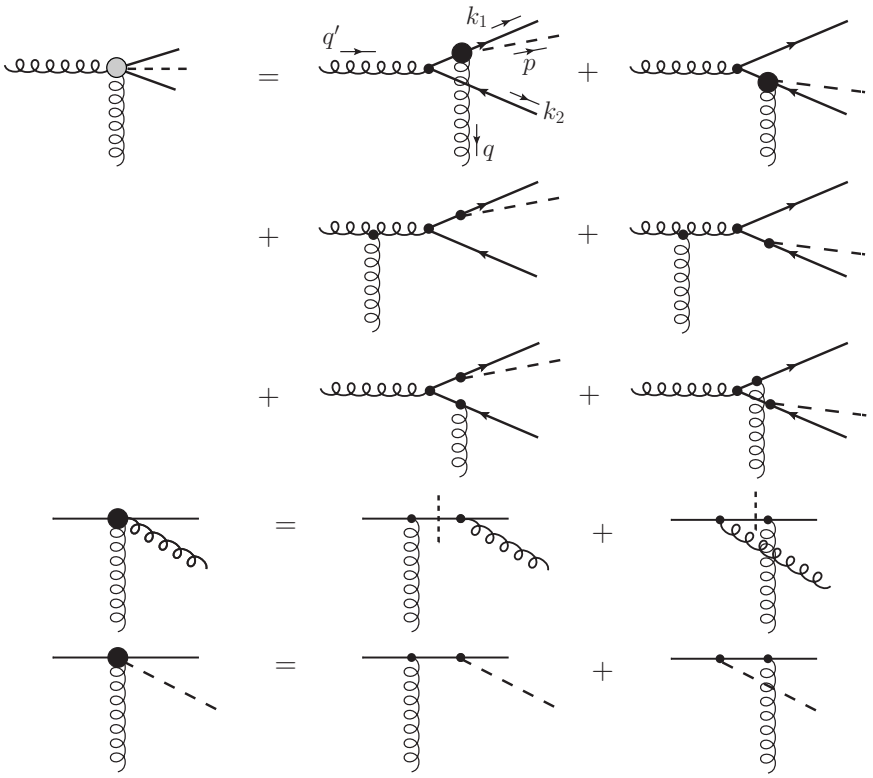

FIG. 2: Explanation for the effective vertices in the Higgsstrahlung process off heavy quarks, which are involved in the graphs in Fig. 1 and 3.

while α, $\vec{\pi}$ and $\vec{q}$ (and hence, Q^2) remain unchanged, as well as the $\bar{Q}Qh$ invariant mass is preserved, $M^2(\beta, \vec{\kappa}; \xi, \vec{p}) = M^2(\beta', \vec{\kappa}'; \xi', \vec{p}')$. The kinematics is now set up and ready for calculation of the amplitudes of $Q\bar{Q}h$ production in hard inelastic quark-proton as well as gluon-proton interactions.

The process of inclusive associated Higgs boson and $Q\bar{Q}$ pair production,

$$q + p \to q + \bar{Q}Q + h + X\,, \tag{2.8}$$

is illustrated by two graphs depicted in Fig. 1 with vertex notations explained in Fig. 2. Similar to production of heavy quarks (see Fig. 2 and Appendix A in Ref. [24]) these graphs can be grouped into two amplitudes attributed to bremsstrahlung (BR) and production (PR) mechanisms, which do, or do not involve the projectile light quarks or gluons, respectively. The BR mechanism includes the same graphs as radiation of a gluon (see Refs. [29, 30]), i.e. interaction with the source parton before and after radiation, and interaction with the radiated gluon. The PR mechanism, responsible for the transition $g \to \bar{Q}Q$, includes the interactions with the gluon and the produced $\bar{Q}Q$. Each of these two combinations is gauge invariant and can be expressed in terms of three-body dipole cross sections, $\sigma_{g\bar{q}q}$ and $\sigma_{g\bar{Q}Q}$ respectively.

$$M_{q,g} = M_{q,g}^{\rm BR} + M_{q,g}^{\rm PR}\,, \tag{2.9}$$

where subscripts q, g denote contributions with hard gluon radiation by the projectile valence or sea quarks and gluons, respectively. The corresponding terms in the amplitude have the

following forms,

$$M^{\mathrm{BR},\lambda_g}_{q,g}(\alpha,\vec{\pi};\beta,\vec{\kappa};\xi,\vec{p};\vec{q}) \simeq \sum_{a,b} f_a(\vec{q}) \tag{2.10}$$
$$\times \Big[\tau^q_a\tau^q_b\Big(\Phi^{\mathrm{BR},\lambda_g}_{q,g}(\alpha,\vec{\pi}+(1-\alpha)\vec{q};\beta,\vec{\kappa};\xi,\vec{p}) - \Phi^{\mathrm{BR},\lambda_g}_{q,g}(\alpha,\vec{\pi}-\alpha\vec{q};\beta,\vec{\kappa};\xi,\vec{p})$$
$$- \Phi^{\mathrm{BR},\lambda_g}_{q,g}(\alpha,\vec{\pi}+(1-\alpha)\vec{q};\beta',\vec{\kappa}\,';\xi',\vec{p}\,') + \Phi^{\mathrm{BR},\lambda_g}_{q,g}(\alpha,\vec{\pi}-\alpha\vec{q};\beta',\vec{\kappa}\,';\xi',\vec{p}\,')\Big)$$
$$+ \tau^q_b\tau^q_a\Big(\Phi^{\mathrm{BR},\lambda_g}_{q,g}(\alpha,\vec{\pi};\beta,\vec{\kappa};\xi,\vec{p}) - \Phi^{\mathrm{BR},\lambda_g}_{q,g}(\alpha,\vec{\pi}+(1-\alpha)\vec{q};\beta,\vec{\kappa};\xi,\vec{p})$$
$$- \Phi^{\mathrm{BR},\lambda_g}_{q,g}(\alpha,\vec{\pi};\beta',\vec{\kappa}\,';\xi',\vec{p}\,') + \Phi^{\mathrm{BR},\lambda_g}_{q,g}(\alpha,\vec{\pi}+(1-\alpha)\vec{q};\beta',\vec{\kappa}\,';\xi',\vec{p}\,')\Big)\Big]\,\mathcal{G}^{Q(g)}_{b(cbd)}\,,$$

$$M^{\mathrm{PR},\lambda_g}_{q,g}(\alpha,\vec{\pi};\beta,\vec{\kappa};\xi,\vec{p};\vec{q}) \simeq \sum_{a,b} f_a(\vec{q})\,\mathcal{G}^{q(g)}_{b(cbd)}$$
$$\times \Big[\tau^Q_a\tau^Q_b\Big(\Phi^{\mathrm{PR},\lambda_g}_{q,g}(\alpha,\vec{\pi}+(1-\alpha)\vec{q};\beta,\vec{\kappa}-\beta\vec{q};\xi,\vec{p})$$
$$- \Phi^{\mathrm{PR},\lambda_g}_{q,g}(\alpha,\vec{\pi}+(1-\alpha)\vec{q};\beta,\vec{\kappa}-\beta\vec{q};\xi,\vec{p}-\xi\vec{q})\Big)$$
$$+ \tau^Q_b\tau^Q_a\Big(\Phi^{\mathrm{PR},\lambda_g}_{q,g}(\alpha,\vec{\pi}+(1-\alpha)\vec{q};\beta',\vec{\kappa}\,'-\beta'\vec{q};\xi',\vec{p}\,')$$
$$- \Phi^{\mathrm{PR},\lambda_g}_{q,g}(\alpha,\vec{\pi}+(1-\alpha)\vec{q};\beta',\vec{\kappa}\,'-\beta'\vec{q};\xi',\vec{p}\,'-\xi'\vec{q})\Big)\Big]\,, \tag{2.11}$$

where $\lambda_g = L, T$ is the hard gluon polarisation, $\mathcal{G}^{q/Q}_b = \tau^{q/Q}_b$ and $\mathcal{G}^g_{cbd} = if_{cbd}$ are the color factors for $q \to g_b q$ and $g_c \to g_b g_d$ splittings, respectively; $L\,(T)$ indicates the longitudinal (transverse) polarisation of the gluon which splits into $\bar{Q}Q$; β', $\vec{\kappa}\,'$; ξ', $\vec{p}\,'$ are defined in Eq. (2.7); $f_a(\vec{q})$ is the amplitude for emission of the t-channel gluon with color index a and transverse momentum $\vec{q}$ by the target proton (summation over gluon color indices a, b is assumed implicitly). In the "production" amplitude $M^{\mathrm{PR},\lambda_g}_{q,g}$ we keep only the leading terms given by two diagrams shown in the first line in Fig. 2. The helicity amplitudes Φ^{λ_g} in Eqs. (2.10), (2.11) read,

$$\Phi^{\mathrm{BR},T}_{q,g}(\alpha,\vec{\pi};\beta,\vec{\kappa};\xi,\vec{p}) = \frac{\sum_{\lambda=\pm1}\Gamma^\lambda_{q,g}(\alpha,\vec{\pi})\,\Gamma^\lambda_Q(\beta,\vec{\kappa})\,\Gamma_H(\xi,\vec{p})}{D_1(\alpha,\vec{\pi};\beta,\vec{\kappa};\xi,\vec{p})\,D_2(\beta,\vec{\kappa};\xi,\vec{p})\,D_5(\xi,\vec{p})}\,, \tag{2.12}$$

$$\Phi^{\mathrm{BR},L}_{q,g}(\alpha,\vec{\pi};\beta,\vec{\kappa};\xi,\vec{p}) = \frac{4\beta(1-\beta)(1-\alpha)M^2(\beta,\vec{\kappa};\xi,\vec{p})\,\Gamma^L_{q,g}\,\Gamma_H(\xi,\vec{p})}{D_1(\alpha,\vec{\pi};\beta,\vec{\kappa};\xi,\vec{p})D_2(\beta,\vec{\kappa};\xi,\vec{p})\,D_5(\xi,\vec{p})}\,, \tag{2.13}$$

$$\Phi^{\mathrm{PR},T}_{q,g}(\alpha,\vec{\pi};\beta,\vec{\kappa};\xi,\vec{p}) = \frac{\sum_{\lambda=\pm1}\Gamma^\lambda_{q,g}(\alpha,\vec{\pi})\,\Gamma^\lambda_Q(\beta,\vec{\kappa})\,\Gamma_H(\xi,\vec{p})}{D_3(\alpha,\vec{\pi})\,D_4(\alpha,\vec{\pi};\beta,\vec{\kappa};\xi,\vec{p})\,D_5(\xi,\vec{p})}\,, \tag{2.14}$$

$$\Phi^{\mathrm{PR},L}_{q,g}(\alpha,\vec{\pi};\beta,\vec{\kappa};\xi,\vec{p}) = \frac{4\beta(1-\beta)(1-\alpha)Q^2(\alpha,\vec{\pi})\,\Gamma^L_{q,g}\,\Gamma_H(\xi,\vec{p})}{D_3(\alpha,\vec{\pi})D_4(\alpha,\vec{\pi};\beta,\vec{\kappa};\xi,\vec{p})\,D_5(\xi,\vec{p})}\,, \tag{2.15}$$

where

$$D_1(\alpha,\vec{\pi};\beta,\vec{\kappa};\xi,\vec{p}) = (1-\alpha)\,[M^2(\beta,\vec{\kappa};\xi,\vec{p}) + Q^2(\alpha,\vec{\pi})]\,,$$
$$D_2(\beta,\vec{\kappa};\xi,\vec{p}) = \beta(1-\beta)M^2(\beta,\vec{\kappa};\xi,\vec{p})\,,$$
$$D_3(\alpha,\vec{\pi}) = (1-\alpha)\,Q^2(\alpha,\vec{\pi})\,,$$
$$D_4(\alpha,\vec{\pi};\beta,\vec{\kappa};\xi,\vec{p}) = \beta(1-\beta)[M^2(\beta,\vec{\kappa};\xi,\vec{p}) + Q^2(\alpha,\vec{\pi})]\,,$$
$$D_5(\xi,\vec{p}) = \xi(1-\xi)[M^2_{Qh}(\xi,\vec{p}) - m^2_Q]\,. \tag{2.16}$$

The amplitudes for gluon emission by the projectile quark q, Γ^λ_q, the gluon splitting into a $Q\bar{Q}$ pair, Γ^λ_Q, and the Higgs boson emission by the heavy Q (or $\bar{Q}$), Γ_H, have the forms,

$$\begin{aligned}
\Gamma^\lambda_q(\alpha,\vec{\pi}) &= \sqrt{\alpha_s(|\vec{\pi}|)}\,\chi^\dagger\left\{(2-\alpha)(\vec{e}_\lambda\cdot\vec{\pi}) + i\alpha[\vec{\sigma}\times\vec{e}_\lambda]\cdot\vec{\pi} + i\alpha^2 m_q\,[\vec{\sigma}\times\vec{e}_\lambda]\cdot\vec{n}\right\}\chi\,,\\
\Gamma^\lambda_Q(\beta,\vec{\kappa}) &= \sqrt{\alpha_s(|\vec{\kappa}|)}\,\phi^\dagger\left\{(1-2\beta)(\vec{\sigma}\cdot\vec{n})(\vec{e}_\lambda\cdot\vec{\kappa}) + i[\vec{e}_\lambda\times\vec{n}]\cdot\vec{\kappa} + m_Q(\vec{\sigma}\cdot\vec{e}_\lambda)\right\}\bar{\phi}\,, \qquad (2.17)\\
\Gamma_H(\xi,\vec{p}) &= \frac{1}{\sqrt{4\pi}}\,\frac{m_Q}{v}\,\xi\,\phi^\dagger\left\{(\vec{\sigma}\cdot\vec{p}) + m_Q\,(2-\xi)(\vec{\sigma}\cdot\vec{n})\right\}\phi\,;
\end{aligned}$$

$v\simeq 246$ GeV is the Higgs vacuum expectation value; and

$$\Gamma^L_q = \sqrt{\alpha_s(|\vec{\pi}|)\,\alpha_s(|\vec{\kappa}|)}\,(1-\alpha)(\chi^\dagger\,\chi)\,(\phi^\dagger\,\vec{\sigma}\cdot\vec{n}\,\bar{\phi})\,. \qquad (2.18)$$

In the above expressions, χ and ϕ are the normalized two-component spinors corresponding to the light q and heavy Q quarks, respectively. Note that the amplitudes (2.10) vanish in the forward direction, $\vec{q}\to 0$.

For the gluon excitation mechanism $g_c\to g_b g_d$ one gets [24],

$$\begin{aligned}
\Gamma^\lambda_g(\alpha,\vec{\pi}) &= 2\sqrt{\alpha_s(|\vec{\pi}|)}\left\{(1-\alpha)(\vec{e}_f\cdot\vec{e}_{in})(\vec{e}_\lambda\cdot\vec{\pi}) + \alpha(\vec{e}_f\cdot\vec{\pi})(\vec{e}_\lambda\cdot\vec{e}_{in})\right.\\
&\left. -\alpha(\vec{e}_{in}\cdot\vec{\pi})(\vec{e}_\lambda\cdot\vec{e}_f)\right\}, \qquad (2.19)\\
\Gamma^L_g &= \sqrt{\alpha_s(|\vec{\pi}|)\,\alpha_s(|\vec{\kappa}|)}\,(\vec{e}_f\cdot\vec{e}_{in})\,(\phi^\dagger\,\vec{\sigma}\cdot\vec{n}\,\bar{\phi})\,. \qquad (2.20)
\end{aligned}$$

where $\vec{e}_{in}$ and $\vec{e}_f$ are incoming and outgoing projectile gluon polarisation vectors, respectively.

The next step is to convert the resulting amplitudes (2.10) and (2.11) into impact parameter representation. In our case, $\vec{\pi}$ and $\vec{p}$ variables acquire shifts proportional to the t-channel gluon momentum $\vec{q}$. Also, due to an interchange $k_1\leftrightarrow k_2$, vector $\vec{p}$ mixes with $\vec{\kappa}$ (cf. Eq. (2.7)). Taking a Fourier transform over $\vec{\pi}$, $\vec{\kappa}$, $\vec{p}$ and $\vec{q}$ variables we arrive at,

$$\tilde{\Phi}^{\lambda_g}_{q,g}(\alpha,\vec{\omega};\beta,\vec{\rho};\xi,\vec{\sigma}) = \frac{1}{(2\pi)^6}\int d^2\vec{\pi}\,d^2\vec{\kappa}\,d^2\vec{p}\,e^{-i\vec{\pi}\cdot\vec{\omega}-i\vec{\kappa}\cdot\vec{\rho}-i\vec{p}\cdot\vec{\sigma}}\,\Phi^{\lambda_g}_{q,g}(\alpha,\vec{\pi};\beta,\vec{\kappa};\xi,\vec{p})\,, \qquad (2.21)$$

and

$$\phi_a(\vec{b}) = \frac{1}{(2\pi)^2}\int d^2\vec{q}\,e^{-i\vec{q}\cdot\vec{b}}\,f_a(\vec{q})\,. \qquad (2.22)$$

In what follows we also use the same notation $\tilde{\Phi}_{q,g}$ for the wave functions in the mixed (momentum-impact parameter) representation with appropriate notations for the arguments. Straightforward calculations lead to,

$$\begin{aligned}
M^{\mathrm{BR},\lambda_g}_{q,g}(\alpha,\vec{\pi};\beta,\vec{\kappa};\xi,\vec{p};\vec{q}) &\simeq \int d^2\vec{\omega}\,d^2\vec{\rho}\,d^2\vec{\sigma}\,d^2b\;e^{i\vec{\pi}\cdot\vec{\omega}+i\vec{\kappa}\cdot\vec{\rho}+i\vec{p}\cdot\vec{\sigma}+i\vec{q}\cdot\vec{b}}\\
&\times\left\{\tau^q_a\tau^q_b\,\tilde{\Phi}^{\mathrm{BR},\lambda_g}_{q,g}(\alpha,\vec{\omega};\beta,\vec{\rho};\xi,\vec{\sigma})\Big[\phi_a(\vec{b}-(1-\alpha)\vec{\omega})-\phi_a(\vec{b}+\alpha\vec{\omega})\Big]\right.\\
&\quad+\tau^q_b\tau^q_a\,\tilde{\Phi}^{\mathrm{BR},\lambda_g}_{q,g}(\alpha,\vec{\omega};\beta,\vec{\rho};\xi,\vec{\sigma})\Big[\phi_a(\vec{b})-\phi_a(\vec{b}-(1-\alpha)\vec{\omega})\Big]\\
&-\quad\left.\{\beta\leftrightarrow\beta',\ \vec{\rho}\leftrightarrow\vec{\rho}',\ \xi\leftrightarrow\xi',\ \vec{\sigma}\leftrightarrow\vec{\sigma}\,'\}\right\}\mathcal{G}^{Q(g)}_{b(cbd)}\,, \qquad (2.23)
\end{aligned}$$

$$M_{q,g}^{\mathrm{PR},\lambda_g}(\alpha,\vec{\pi};\beta,\vec{\kappa};\xi,\vec{p};\vec{q}) \simeq \mathcal{G}_{b(cbd)}^{q(g)} \int d^2\vec{\omega}\, d^2\vec{\rho}\, d^2\vec{\sigma}\, d^2b\, e^{i\vec{\pi}\cdot\vec{\omega}+i\vec{\kappa}\cdot\vec{\rho}+i\vec{p}\cdot\vec{\sigma}+i\vec{q}\cdot\vec{b}}$$
$$\times \Big\{\tau_a^Q \tau_b^Q\, \tilde{\Phi}_{q,g}^{\mathrm{PR},\lambda_g}(\alpha,\vec{\omega};\beta,\vec{\rho};\xi,\vec{\sigma})\Big[\phi_a(\vec{b}-(1-\alpha)\vec{\omega}+\beta\vec{\rho})$$
$$-\phi_a(\vec{b}-(1-\alpha)\vec{\omega}+\beta\vec{\rho}+\xi\vec{\sigma})\Big]$$
$$+\{a\leftrightarrow b,\ \beta\leftrightarrow\beta',\ \vec{\rho}\leftrightarrow\vec{\rho}',\ \xi\leftrightarrow\xi',\ \vec{\sigma}\leftrightarrow\vec{\sigma}\,'\}\Big\}, \tag{2.24}$$

where

$$\vec{\rho}\,' = -\frac{\beta\vec{\rho}+\xi\vec{\sigma}}{\xi+\beta(1-\xi)}, \qquad \vec{\sigma}\,' = (1-\xi)\vec{\sigma}-\vec{\rho}. \tag{2.25}$$

Notice that the amplitude (2.24) vanishes at $\xi \to 0$. Let us now turn to discussion of the diffractive Higgsstrahlung amplitudes at the hadronic level.

III. DIFFRACTIVE HIGGSSTRAHLUNG OFF HEAVY QUARKS

Consider the single diffractive heavy quark pair production, with subsequent Higgsstrahlung off a heavy quark or antiquark, in a proton-proton collision, i.e.

$$p + p \to (\bar{Q}Qh) + X + p\,. \tag{3.1}$$

Further in this Section, we perform an analysis of the amplitudes and observables for this process within the color dipole approach [24].

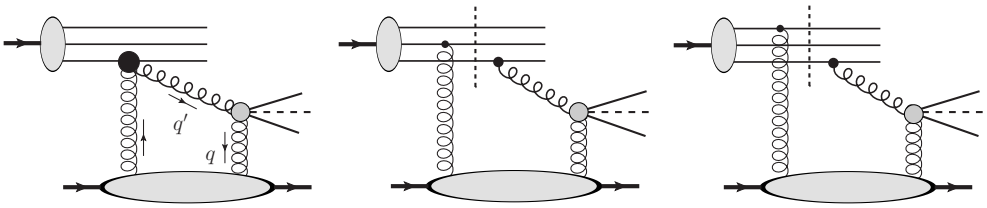

FIG. 3: The dominating contributions to the diffractive Higgsstrahlung off heavy quarks. Parton-level subprocesses denoted by filled large grey and bold circles are described separately in Fig. 2.

The diffractive amplitude can be represented via the optical theorem in terms of amplitudes of inelastic (anti)quark and gluon interaction off the proton target derived in the previous section, as is depicted in Fig. 3. Here, the leading contributions coming from diffractive excitation of valence or sea (anti)quarks are shown. Practically, the important subprocesses are the hard (virtual) gluon Bremsstrahlung $q \to q + g^*$, the gluon-gluon fusion into a heavy $Q\bar{Q}$ pair $g^*g \to Q\bar{Q}$ (g comes with the target proton) with subsequent Higgs boson radiation of a heavy quark Q or antiquark $\bar{Q}$, e.g. $Q \to Q + h$, as is depicted in Fig. 2. We neglect the contributions coming from the virtual gluon splitting into the $Q\bar{Q}+h$ system, which is strongly suppressed compared to the gg-fusion by the large gluon virtuality as was demonstrated in Ref. [24]. Furthermore, the second (color neutralizing) cross-channel gluon can couple either to the same (valence or sea) quark or antiquark, which emits the hard gluon, or to a spectator parton in the proton wave function. The latter contributions are

thus sensitive to soft hadron-scale separations between proton constituents, which strongly breaks down diffractive factorisation, similarly to the diffractive Abelian radiation [21, 22].

Let the hard gluon be emitted by one of the projectile partons, a quark or a gluon, labeled as q_1, with momentum fraction $x_q \equiv x_q^1$ (predominantly, a valence quark for large $x_q \to 1$ and a sea quark or a gluon for small $x_q \ll 1$). Due to the hard emission the projectile parton q_1 position in impact parameter plane, being initially $\vec{r}_1$, gets shifted by a small amount given by the hard scale of the process to $\vec{r}_1 + \alpha\vec{\omega}$. This leads to a change in the interaction strength, because dipoles with different sizes interact differently. The interference between the amplitudes at different impact parameters gives rise to the diffractive scattering. Below, we illustrate basic derivations in the case of diffractive quark excitation, while the gluon excitation can be evaluated similarly.

Here, we employ the dominant amplitude for the inclusive $Q\bar{Q}h$-production process $qp(gp) \to (Q\bar{Q}h) + X$ in impact parameter representation, given by Eq. (2.24), for construction of the corresponding diffractive amplitude. This can be done by attaching the second *"screening"* gluon between the projectile quarks and the target, and then applying the optical theorem to the partial elastic amplitude

$$2\,\mathrm{Im}\, f_{el}(\vec{b},\vec{r}) = \frac{1}{N_c}\sum_X \sum_{c_f c_i} \left|V_q(\vec{b}) - V_q(\vec{b}+\vec{r})\right|^2, \qquad \int d^2\vec{b}\;\; 2\mathrm{Im} f_{el}(\vec{b},\vec{r}) = \sigma(\vec{r})\,, \quad (3.2)$$

for dipole of transverse size r colliding with a proton at impact parameter b, which is specified below. In Eq. (3.2), $\sigma(\vec{r})$ is the universal dipole cross section known from phenomenology (see e.g.[26]), $V_q(\vec{b}) \sim \tau^a \phi_a(\vec{b})$ is the quark-target interaction amplitude where summation over t-channel gluon colors, as well as averaging and summation over the initial and final quark quantum numbers, respectively, is implied, and $\phi_a(\vec{b})$ is given by Eq. (5.10) (for more details, see Ref. [22]). The "screening" gluon can be attached either to the quark q_1, which emits the hard gluon, or to a different spectator parton in the projectile proton, e.g. to a valence quark q_j, $j = 2, 3$, separated from the first one by $\vec{r}_{1j} = \vec{r}_j - \vec{r}_1$. Following this procedure, in our case we arrive at the following diffractive amplitudes in the forward limit,

$$\begin{aligned}
&\Sigma^{\lambda_g}_{q(1)}\big(\vec{r}_1,\vec{r}_2,\vec{r}_3;\alpha,\vec{\omega};\beta,\vec{\rho};\xi,\vec{\sigma}\big) = \frac{1}{2}\,(\tau_b^{q_1}\tau_a^{q_1})(\tau_a^Q\tau_b^Q)\,\Big\{\tilde{\Phi}_q^{\mathrm{PR},\lambda_g}(\alpha,\vec{\omega};\beta,\vec{\rho};\xi,\vec{\sigma})\\
&\times \int d^2b\,\Big\{\Big[2\mathrm{Im}\, f_{el}(\vec{b},(1-\alpha)\,\vec{\omega}-\xi\vec{\sigma}) - 2\mathrm{Im}\, f_{el}(\vec{b},(1-\alpha)\,\vec{\omega})\Big]\\
&-\Big[2\mathrm{Im}\, f_{el}(\vec{b},(1-\alpha)\,\vec{\omega}-\beta\vec{\rho}-\xi\vec{\sigma}) - 2\mathrm{Im}\, f_{el}(\vec{b},(1-\alpha)\,\vec{\omega}-\beta\vec{\rho})\Big]\Big\}\\
&+\tilde{\Phi}_q^{\mathrm{PR},\lambda_g}(\alpha,\vec{\omega};\beta',\vec{\rho}\,';\xi',\vec{\sigma}\,')\int d^2b\,\Big\{\Big[2\mathrm{Im}\, f_{el}(\vec{b},\vec{\omega}-\xi'\vec{\sigma}\,') - 2\mathrm{Im}\, f_{el}(\vec{b},\vec{\omega})\Big]\\
&-\Big[2\mathrm{Im}\, f_{el}(\vec{b},\vec{\omega}-\beta'\vec{\rho}\,'-\xi'\vec{\sigma}\,') - 2\mathrm{Im}\, f_{el}(\vec{b},\vec{\omega}-\beta'\vec{\rho}\,')\Big]\Big\}\\
&+\frac{1}{2}\,(\tau_b^{q_1}\tau_a^{q_1})(\tau_b^Q\tau_a^Q)\,\Big\{\tilde{\Phi}_q^{\mathrm{PR},\lambda_g}(\alpha,\vec{\omega};\beta,\vec{\rho};\xi,\vec{\sigma})\int d^2b\,\Big\{\Big[2\mathrm{Im}\, f_{el}(\vec{b},\vec{\omega}-\xi\vec{\sigma}) - 2\mathrm{Im}\, f_{el}(\vec{b},\vec{\omega})\Big]\\
&-\Big[2\mathrm{Im}\, f_{el}(\vec{b},\vec{\omega}-\beta\vec{\rho}-\xi\vec{\sigma}) - 2\mathrm{Im}\, f_{el}(\vec{b},\vec{\omega}-\beta\vec{\rho})\Big]\Big\} + \tilde{\Phi}_q^{\mathrm{PR},\lambda_g}(\alpha,\vec{\omega};\beta',\vec{\rho}\,';\xi',\vec{\sigma}\,')\\
&\times \int d^2b\,\Big\{\Big[2\mathrm{Im}\, f_{el}(\vec{b},(1-\alpha)\vec{\omega}-\xi'\vec{\sigma}\,') - 2\mathrm{Im}\, f_{el}(\vec{b},(1-\alpha)\vec{\omega})\Big]\\
&-\Big[2\mathrm{Im}\, f_{el}(\vec{b},(1-\alpha)\vec{\omega}-\beta'\vec{\rho}\,'-\xi'\vec{\sigma}\,') - 2\mathrm{Im}\, f_{el}(\vec{b},(1-\alpha)\vec{\omega}-\beta'\vec{\rho}\,')\Big]\Big\}\Big\}\,, \qquad (3.3)
\end{aligned}$$

$$
\begin{aligned}
&\Sigma^{\lambda_g}_{q(j=2,3)}\big(\vec{r}_1,\vec{r}_2,\vec{r}_3;\alpha,\vec{\omega};\beta,\vec{\rho};\xi,\vec{\sigma}\big) = (\tau_b^{q_1}\tau_a^{q_j})(\tau_a^Q\tau_b^Q)\,\tilde{\Phi}_q^{\mathrm{PR},\lambda_g}(\alpha,\vec{\omega};\beta,\vec{\rho};\xi,\vec{\sigma})\\
&\times\int d^2b\,\Big\{\Big[2\mathrm{Im}\,f_{el}(\vec{b},\vec{r}_{1j}-(1-\alpha)\,\vec{\omega}+\beta\vec{\rho})-2\mathrm{Im}\,f_{el}(\vec{b},\vec{r}_{1j}-(1-\alpha)\vec{\omega}+\beta\vec{\rho}+\xi\vec{\sigma})\Big]\\
&\qquad-\Big[2\mathrm{Im}\,f_{el}(\vec{b},\vec{r}_{1j}-(1-\alpha)\,\vec{\omega})-2\mathrm{Im}\,f_{el}(\vec{b},\vec{r}_{1j}-(1-\alpha)\vec{\omega}+\xi\vec{\sigma})\Big]\Big\}\\
&+(\tau_b^{q_1}\tau_a^{q_j})(\tau_b^Q\tau_a^Q)\,\tilde{\Phi}_q^{\mathrm{PR},\lambda_g}(\alpha,\vec{\omega};\beta',\vec{\rho}\,';\xi',\vec{\sigma}\,')\\
&\times\int d^2b\,\Big\{\Big[2\mathrm{Im}\,f_{el}(\vec{b},\vec{r}_{1j}-(1-\alpha)\,\vec{\omega}+\beta'\vec{\rho}\,')-2\mathrm{Im}\,f_{el}(\vec{b},\vec{r}_{1j}-(1-\alpha)\vec{\omega}+\beta'\vec{\rho}\,'+\xi'\vec{\sigma}\,')\Big]\\
&\qquad-\Big[2\mathrm{Im}\,f_{el}(\vec{b},\vec{r}_{1j}-(1-\alpha)\,\vec{\omega})-2\mathrm{Im}\,f_{el}(\vec{b},\vec{r}_{1j}-(1-\alpha)\vec{\omega}+\xi'\vec{\sigma}\,')\Big]\Big\}\,, \qquad (3.4)
\end{aligned}
$$

which correspond to the left, middle and right diagrams in Fig. 3, respectively. In the above formulas, τ_a^q and τ_a^Q are the Gell-Mann matrices of gluon couplings to a light (valence/sea) quark and to a heavy quark, respectively. The total diffractive Higgsstrahlung amplitude is a sum of the above contributions,

$$
\Sigma_q^{\lambda_g} = \sum_{j=1,2,3}\Sigma^{\lambda_g}_{q(j)} + \text{ quark permutations}\,, \qquad (3.5)
$$

and similarly for gluon excitations with a proper color factor. In the above expressions we implicitly sum over gluon colors a, b. Factor $1/2$ in $\Sigma^{\lambda_g}_{q(1)}$ comes from the averaging over t-channel gluon momenta interchanges. As expected, the effective elastic amplitudes are proportional to the difference between elastic amplitudes for the dipoles of slightly different sizes induced by hard bremsstrahlung processes. Such an interference results in the interplay between hard and soft fluctuations in diffractive pp scattering, making the breakdown of diffractive factorisation significant [21, 22]. Now we are in a position to derive the inclusive and single diffractive Higgsstrahlung cross sections at the hadronic level.

IV. HIGGSSTRAHLUNG CROSS SECTIONS AT HADRONIC LEVEL

A. Inclusive Higgsstrahlung

Transition to the hadron level is normally achieved by invoking the initial proton Ψ_i and proton remnant Ψ_f wave functions which encode information about kinematics and probability distributions of individual partons. In the unobservable part, the completeness relation to the wave function of the proton remnant in the final state reads

$$
\begin{aligned}
&\sum_f \Psi_f(\vec{r}_1,\vec{r}_2,\vec{r}_3;\{\vec{r}_q^{\,1,2,\dots},x_q^{1,2,\dots}\};\{\vec{r}_g^{\,1,2,\dots},x_g^{1,2,\dots}\})\\
&\qquad\times\,\Psi_f^*(\vec{r}\,'_1\,\vec{r}\,'_2,\vec{r}\,'_3;\{\vec{r}_q^{\,\prime 1,2,\dots},x_q^{\prime 1,2,\dots}\};\{\vec{r}_g^{\,\prime 1,2,\dots},x_g^{\prime 1,2,\dots}\})\\
&\qquad=\,\delta\big(\vec{r}_1-\vec{r}\,'_1\big)\delta(\vec{r}_2-\vec{r}\,'_2)\delta(\vec{r}_3-\vec{r}\,'_3)\prod_j\delta(\vec{r}_{q/g}^{\,j}-\vec{r}_{q/g}^{\,\prime j})\delta(x^j_{q/g}-x^{\prime j}_{q/g})\,, \qquad (4.1)
\end{aligned}
$$

where $\vec{r}_{q/g}^{\,i}$, $x^i_{q/g}$ are the transverse coordinates and fractional light-cone momenta of the valence/sea quarks and gluons.

The light-cone partonic wave function of the initial proton depends on transverse coordinates and fractional momenta of of all valence and sea quarks and gluons. We assume

that the mean transverse distance between a source valence quark and the sea quarks or gluons is much smaller than the mean distance between the valence quarks. Such a two-scale structure of the proton is supported by numerous evidences in theoretical and experimental observations [31]. Therefore the transverse positions of sea quarks and gluons can be identified with the coordinates of the valence quarks, and the proton wave function can be parametrized as,

$$|\Psi_i(\vec{r}_1,\vec{r}_2,\vec{r}_3;x_q,\{x_q^{2,3,\cdots}\},\{x_g^{1,2,\cdots}\})|^2 \;=\; \frac{3a^2}{\pi^2}e^{-a(r_1^2+r_2^2+r_3^2)}\rho(x_q,\{x_q^{2,3,\cdots}\},\{x_g^{1,2,\cdots}\}) \\ \times\; \delta(\vec{r}_1+\vec{r}_2+\vec{r}_3)\delta(1-x_q-\sum_j x_{q/g}^j), \qquad (4.2)$$

where the summation is taken over all the valence and sea quarks and gluons not participating in the hard interaction. For simplicity, we parameterize the valence part of the proton wave function in the form of symmetric Gaussian for the spacial quark distributions. Other notations in (4.2), the variable $x_q^1 \equiv x_q = x_1/\alpha$ is defined as the light-cone fraction of the quark emitting the hard gluon; x_1 is the hard gluon momentum fraction; $a = \langle r_{ch}^2\rangle^{-1}$ is the inverse proton mean charge radius squared; ρ is a valence/sea (anti)quark distribution function in the projectile proton. Notice that this distribution has a low scale, so the constituent quarks, i.e. the valence quarks together with the sea and gluons they generate, carry the whole momentum of the proton.

In the case of diffractive quark excitations, after integration over the fractional momenta of all partons not participating in the hard interaction, we arrive at a single valence/sea (anti)quark distribution in the proton, probed by the hard gluon radiation process,

$$\int\prod_{j\neq 1}dx_q^j\prod_k dx_g^k\,\delta\left(1-x_q-\sum_j x_{q/g}^j\right)\rho\left(x_q,\{x_q^{2,3,\cdots}\},\{x_g^{1,2,\cdots}\}\right)=\rho_{(\bar{q})q}(x_q)\,, \qquad (4.3)$$

where $(\bar{q})q$ denotes the sea/valence (anti)quark having fractional momentum x_q. In the case of diffractive excitation of a gluon, instead of the quark densities $\rho_q(x)$ we use $(9/4)^2 g(x)$ accounting for projectile gluon density $g(x)$ with a proper color factor.

While single diffraction with production of $Q\bar{Q}$ and hence $Q\bar{Q}h$ is dominated by glue-glue fusion ("production"), in the corresponding inclusive process the "bremsstrahlung" contribution can also be important [24]. The differential cross section for the inclusive $Q\bar{Q}h$ production in pp collisions,

$$\frac{d\sigma_{incl}^{\lambda_g}(pp\to(Q\bar{Q}h)X)}{dx_F} \;=\; \frac{x_1}{x_1+x_2}\int_{x_1}^1\frac{d\alpha}{\alpha^2}\times \\ \sum_q\left[\rho_q\Big(\frac{x_1}{\alpha},\mu^2\Big)+\rho_{\bar{q}}\Big(\frac{x_1}{\alpha},\mu^2\Big)\right]\frac{d\sigma^{\lambda_g}(qp\to(Q\bar{Q}h)X)}{d\ln\alpha}\,, \qquad (4.4)$$

is expressed via $Q\bar{Q}h$ production cross section in qp scattering, neglecting the higher-twist bremsstrahlung-production interference terms [24]

$$\frac{d\sigma^{\lambda_g}(qp\to(Q\bar{Q}h)X)}{d\ln\alpha} \;\simeq\; \frac{d\sigma_{\rm BR}^{\lambda_g}}{d\ln\alpha}+\frac{d\sigma_{\rm PR}^{\lambda_g}}{d\ln\alpha}\,,$$

where $x_{1,2} = q'^{\pm}/P_{1,2}^+$ are the $Q\bar{Q}h$ system longitudinal momentum fractions, P_1 is the 4-momentum of the projectile proton, q' is the 4-momentum of the hard gluon, $x_F = x_1 - x_2$

is the standard Feynman variable. The hard scale μ^2 and the momentum fraction x_1 can be expressed in terms of phase space variables M^2, x_F as,

$$\tau \simeq \frac{M^2}{s}\,, \qquad x_1 = \frac{1}{2}\Big(\sqrt{x_F^2+4\tau}+x_F\Big)\,, \qquad \mu^2 \simeq (1-x_1)M^2\,,$$

for not very large transverse momenta of the produced $Q\bar{Q}h$ system.

The bremsstrahlung contribution to the inclusive Higgsstrahlung cross section (4.5) is given by

$$\begin{aligned}
\frac{d\sigma^{\lambda_g}_{\rm BR}(qp\to(Q\bar{Q}h)X)}{d\ln\alpha\, d\ln\beta\, d\ln\xi} &= \frac{1}{(2\pi)^4}\int d^2\vec{\kappa}\, d^2\vec{p}\int d^2\vec{\omega}\,\Big\{|\tilde{\Phi}^{\lambda_g}_{\rm BR}(\alpha,\vec{\omega};\beta,\vec{\kappa};\xi,\vec{p})|^2 \\
&\quad + |\tilde{\Phi}^{\lambda_g}_{\rm BR}(\alpha,\vec{\omega};\beta',\vec{\kappa}\,';\xi',\vec{p}\,')|^2\Big\}\,\Sigma_{\rm BR}(\alpha,\vec{\omega})\,, \\
\Sigma_{\rm BR}(\alpha,\vec{\omega}) &= \frac{9}{8}\Big[\sigma_{\bar{q}q}(\vec{\omega})+\sigma_{\bar{q}q}[(1-\alpha)\vec{\omega}]\Big]-\frac{1}{8}\,\sigma_{\bar{q}q}(\alpha\vec{\omega})\,, \qquad (4.5)
\end{aligned}$$

where $\tilde{\Phi}^{\lambda_g}_{\rm BR}(\alpha,\vec{\omega};\beta,\vec{\kappa};\xi,\vec{p})$ is the bremsstrahlung wave function for the hard $q/g\to(Q\bar{Q}h)+q/g$ process in the mixed representation. Note, the higher-twist interference terms between Higgsstrahlung amplitudes with the Higgs boson coupled to a quark and to an antiquark were neglected in this analysis.

On analogy, the production contribution for the inclusive Higgsstrahlung cross section (4.5) reads

$$\begin{aligned}
\frac{d\sigma^{\lambda_g}_{\rm PR}(qp\to(Q\bar{Q}h)X)}{d\ln\alpha\, d\ln\beta\, d\ln\xi} &= \frac{1}{(2\pi)^2}\int d^2\vec{\pi}\int d^2\vec{\rho}\, d^2\vec{\sigma}\,\Big\{|\tilde{\Phi}^{\lambda_g}_{\rm PR}(\alpha,\vec{\pi};\beta,\vec{\rho};\xi,\vec{\sigma})|^2\,\Sigma_{\rm PR}(\beta,\vec{\rho};\xi,\vec{\sigma}) \\
&\quad + \ |\tilde{\Phi}^{\lambda_g}_{\rm PR}(\alpha,\vec{\pi};\beta',\vec{\rho}\,';\xi',\vec{\sigma}\,')|^2\,\Sigma_{\rm PR}(\beta',\vec{\rho}\,';\xi',\vec{\sigma}\,')\Big\}\,, \\
\Sigma_{\rm PR}(\beta,\vec{\rho};\xi,\vec{\sigma}) &= \frac{9}{8}\Big[\sigma_{\bar{q}q}(\beta\vec{\rho}+\xi\vec{\sigma})-\sigma_{\bar{q}q}(\beta\vec{\rho}\,)\Big]-\frac{1}{8}\Big[\sigma_{\bar{q}q}(\vec{\rho}+\xi\vec{\sigma})-\sigma_{\bar{q}q}(\vec{\rho})\Big]\,, \qquad (4.6)
\end{aligned}$$

where $\tilde{\Phi}^{\lambda_g}_{\rm PR}(\alpha,\vec{\omega};\beta,\vec{\kappa};\xi,\vec{p})$ is the production wave function for the hard $q/g+g\to(Q\bar{Q}h)+q/g$ process in the mixed representation.

B. Single diffractive Higgsstrahlung

The single diffractive $Q\bar{Q}h$ production cross section takes the following form

$$\begin{aligned}
&\frac{d\sigma^{\lambda_g}_{sd}(pp\to p(Q\bar{Q}h)X)}{d^2\vec{\kappa}\, d^2\vec{p}\, d\ln\alpha\, d\ln\beta\, d\ln\xi\, d^2\delta_\perp}\Big|_{\delta_\perp\to 0} = \frac{1}{(2\pi)^4}\frac{9}{256\pi^2}\sum_{l=q,\,g}\int dx_q\,\Big[\rho_q(x_q,\mu^2)+\rho_{\bar{q}}(x_q,\mu^2)\Big] \\
&\int d^2\vec{r}_1 d^2\vec{r}_2 d^2\vec{r}_3\, d^2\vec{\omega}\, d^2\vec{\rho}_1 d^2\vec{\rho}_2\, d^2\vec{\sigma}_1 d^2\vec{\sigma}_2\, e^{i\vec{\kappa}\cdot(\vec{\rho}_1-\vec{\rho}_2)}e^{i\vec{p}\cdot(\vec{\sigma}_1-\vec{\sigma}_2)} \\
&\times\Sigma^{\lambda_g}_l\big(\vec{r}_1,\vec{r}_2,\vec{r}_3;\alpha,\vec{\omega};\beta,\vec{\rho}_1;\xi,\vec{\sigma}_1\big)\Sigma^{\lambda_g *}_l\big(\vec{r}_1,\vec{r}_2,\vec{r}_3;\alpha,\vec{\omega};\beta,\vec{\rho}_2;\xi,\vec{\sigma}_2\big)\,, \qquad (4.7)
\end{aligned}$$

where $\Sigma^{\lambda_g}_{q,g}$ is the diffractive amplitude defined in Eq. (3.5), $\vec{\pi}$ is integrated out as an unobservable momentum, the summation is performed over all valence/sea quarks and gluons in the proton. Note, the differential cross section Eq. (4.7) is the full expression, which

includes by default the effects of absorption at the amplitude level via differences of elastic amplitudes fitted to data, and does not need any extra survival probability factor. This fact has been advocated in detail in Ref. [23], and we do not repeat this discussion here.

For further calculations in Eq. (4.7) we have choosen as phase space variables the transverse momentum of the recoil heavy (anti)quark, $\vec{\kappa}$; the Higgs boson transverse momentum, $\vec{p}$. The other variables are the longitudinal momentum fraction of the $Q\bar{Q}h$ system, α; of one of the quarks, β; and of the Higgs boson, ξ. Later on, when it comes to the actual measurements, another set of variables and corresponding differential distributions can be considered. For example, in practice it can be useful to convert the phase space variables $\{\alpha, x_q, \dots\}$ to another convenient set $\{\alpha, x_1, \dots\}$ as follows,

$$\frac{d\alpha dx_q}{\alpha} = \frac{dx_1 dx_q}{x_1} = -\frac{dx_1 d\alpha}{\alpha^2}\,.$$

The dipole elastic amplitude $f_{el}(\vec{b}, \vec{r})$, which enters the diffractive Higgsstrahlung amplitudes Σ^{λ_g}, implicitly depends on energy. It cannot be calculated reliably from the first principles, but is known from phenomenology. Since large dipole sizes $|\vec{r}_i - \vec{r}_j| \sim b \sim R_p$, $i \neq j$ (R_p is the mean proton size) are important in Eq. (4.7), the Bjorken variable x is ill defined, and a more appropriate variable is the collisions energy. A parametrization of the dipole cross section as a function of the c.m. energy squared s, was proposed and fitted to data in Ref. [25], and the corresponding partial dipole amplitude is given by [32–34]

$$\begin{aligned}\mathrm{Im} f_{el}(\vec{b}, \vec{r}_p) = \frac{\sigma_0(s)}{8\pi\mathcal{B}(s)}\Bigg\{ &\exp\left[-\frac{[\vec{b} + \vec{r}_p(1-x_q)]^2}{2\mathcal{B}(s)}\right] + \exp\left[-\frac{[\vec{b} + \vec{r}_p x_q]^2}{2\mathcal{B}(s)}\right] \\ &- 2\exp\left[-\frac{r_p^2}{R_0^2(s)} - \frac{[\vec{b} + \vec{r}_p(1/2 - x_q)]^2}{2\mathcal{B}(s)}\right]\Bigg\}, \quad \mathcal{B}(s) = R_N^2(s) + R_0^2(s)/8\,, \end{aligned} \tag{4.8}$$

where x_q is the light-cone momentum fraction of the quark in the dipole defined in Eq. (4.2), and

$$\begin{aligned} R_0(s) = 0.88\,\mathrm{fm}\,(s_0/s)^{0.14}\,, \quad R_N^2(s) = B_{el}^{\pi p}(s) - \frac{1}{4}R_0^2(s) - \frac{1}{3}\langle r_{ch}^2\rangle_\pi\,, \\ \sigma_0(s) = \sigma_{tot}^{\pi p}(s)\Big(1 + \frac{3R_0^2(s)}{8\langle r_{ch}^2\rangle_\pi}\Big)\,. \end{aligned} \tag{4.9}$$

Here, the pion-proton total cross section is parameterized as [35] $\sigma_{tot}^{\pi p}(s) = 23.6(s/s_0)^{0.08}$ mb, $s_0 = 1000$ GeV^2, the mean pion radius squared is [36] $\langle r_{ch}^2\rangle_\pi = 0.44$ fm^2. We employ the Regge parametrization of the elastic slope $B_{el}^{\pi p}(s) = B_0 + 2\alpha'_{I\!P}\ln(s/\mu^2)$, with $B_0 = 6$ GeV^{-2}, $\alpha'_{I\!P} = 0.25$ GeV^{-2}, and $\mu^2 = 1$ GeV^2; and the s-dependent parametrization (4.8) with (4.9) in numerical analysis of the diffractive Higgsstrahlung which is controlled essentially by soft interactions (or large hadron-scale dipoles).

The hard length scales controlling the the process of heavy $Q\bar{Q}h$ system production, $\langle\rho^2\rangle \sim 1/m_Q^2$ and $\langle\sigma^2\rangle \sim 1/M_h^2$, are much smaller than any of the hadronic scales $\sim \langle R\rangle^2$. Another length scale for the mechanism under consideration, $\langle\omega^2\rangle \sim 1/m_q^2 \sim \langle R\rangle^2$, is soft for light valence/sea quarks in the proton wave function [24]. In the forward limit $\delta_\perp \to 0$, the b-dependence comes only into the partial dipole amplitude f_{el} defined in Eq. (4.8), so it

can be integrated out in the cross section (4.7). Relying on the smallness of the hard length scales, σ, $\rho \ll r_{ij} = |\vec{r}_i - \vec{r}_j| \sim \omega \sim R$, we can write,

$$\Big[\mathrm{Im}\, f_{el}(\vec{b}, \vec{R} + A\vec{\rho} + B\vec{\sigma}) - \mathrm{Im}\, f_{el}(\vec{b}, \vec{R} + A\vec{\rho})\Big] - \Big[\mathrm{Im}\, f_{el}(\vec{b}, \vec{R} + B\vec{\sigma}) - \mathrm{Im}\, f_{el}(\vec{b}, \vec{R})\Big]$$
$$\simeq A\, B\, \frac{\partial^2 \mathrm{Im}\, f_{el}(\vec{b}, \vec{x})}{\partial x_i \partial x_j}\Big|_{\vec{x}=\vec{R}} \rho_i\, \sigma_j\,, \tag{4.10}$$

where,

$$\int d^2b\, \frac{\partial^2 \mathrm{Im}\, f_{el}(\vec{b}, \vec{x})}{\partial x_i \partial x_j}\Big|_{\vec{x}=\vec{R}} \equiv C_{ij}(\vec{R})\,,$$
$$C_{ij}(\vec{R}) = \frac{\sigma_0(s)}{R_0^2(s)}\, e^{-R^2/R_0^2(s)} \left[\delta_{ij} - \frac{2R_i R_j}{R_0^2(s)}\right]. \tag{4.11}$$

So one can derive an approximate analytic formulae for the diffractive amplitudes Σ^{λ_g}, which allow to perform analytically the corresponding inverse Fourier transformations in Eq. (4.7) for each helicity amplitude as follows,

$$\int d^2\vec{\rho}\, d^2\vec{\sigma}\, e^{i\vec{\kappa}\cdot\vec{\rho} + i\vec{p}\cdot\vec{\sigma}} \sum_{i,j} C_{ij}(\vec{R})\, \rho_i\, \sigma_j\, \tilde{\Phi}^{\lambda_g}_{q,g}(\alpha, \vec{\omega}; \beta, \vec{\rho}; \xi, \vec{\sigma})$$
$$= (-i)^2 \sum_{i,j} C_{ij}(\vec{R})\, \frac{\partial}{\partial \kappa_i} \frac{\partial}{\partial r_j}\, \Omega^{\lambda_g}_{q,g}(\alpha, \vec{\omega}; \beta, \vec{\kappa}; \xi, \vec{p})\,, \tag{4.12}$$

$$\Omega^{\lambda_g}_{q,g}(\alpha, \vec{\omega}; \beta, \vec{\kappa}; \xi, \vec{p}) \equiv \int \frac{d^2\vec{\pi}}{(2\pi)^2}\, e^{-i\vec{\pi}\cdot\vec{\omega}} \Phi^{\lambda_g}_{q,g}(\alpha, \vec{\pi}; \beta, \vec{\kappa}; \xi, \vec{p})\,, \tag{4.13}$$

where $\Phi^{\lambda_g}_{q,g}$ are defined in Eqs. (2.14) and (2.15), so that only one Fourier transform of the hard scattering amplitude over $\vec{\pi}$ needs to be performed. This significantly simplifies the further calculations, allowing for an efficient analytical analysis. Indeed, the integration over $\vec{s}$ in Eq. (4.7) becomes straightforward,

$$\int d^2\vec{\rho}\, d^2\vec{\sigma}\, e^{i\vec{\kappa}\cdot\vec{\rho} + i\vec{p}\cdot\vec{\sigma}}\, \Sigma^{\lambda_g}_q\big(\vec{r}_1, \vec{r}_2, \vec{r}_3; \alpha, \vec{\omega}; \beta, \vec{\rho}; \xi, \vec{\sigma}\big) \simeq \tag{4.14}$$
$$\chi^q_1(\vec{\omega})(\tau_b^{q_1}\tau_a^{q_1})(\tau_a^Q\tau_b^Q) + \chi^q_2(\vec{\omega})(\tau_b^{q_1}\tau_a^{q_1})(\tau_b^Q\tau_a^Q) + \tag{4.15}$$
$$\chi^q_3(\vec{r}_{12}, \vec{\omega})(\tau_b^{q_1}\tau_a^{q_2})(\tau_a^Q\tau_b^Q) + \chi^q_4(\vec{r}_{12}, \vec{\omega})(\tau_b^{q_1}\tau_a^{q_2})(\tau_b^Q\tau_a^Q) +$$
$$\chi^q_3(\vec{r}_{13}, \vec{\omega})(\tau_b^{q_1}\tau_a^{q_3})(\tau_a^Q\tau_b^Q) + \chi^q_4(\vec{r}_{13}, \vec{\omega})(\tau_b^{q_1}\tau_a^{q_3})(\tau_b^Q\tau_a^Q)\,,$$

where the amplitudes χ^q_i, $i = 1, \ldots, 4$ are defined as,

$$\chi^q_1(\vec{\omega}) = \beta\xi \sum_{i,j} C_{ij}((1-\alpha)\vec{\omega})\, \frac{\partial}{\partial \kappa_i} \frac{\partial}{\partial p_j}\, \Omega^{\lambda_g}_q(\alpha, \vec{\omega}; \beta, \vec{\kappa}; \xi, \vec{p})$$
$$+ \beta'\xi' \sum_{i,j} C_{ij}(\vec{\omega})\, \frac{\partial}{\partial \kappa'_i} \frac{\partial}{\partial p'_j}\, \Omega^{\lambda_g}_q(\alpha, \vec{\omega}; \beta', \vec{\kappa}\,'; \xi', \vec{p}\,')\,, \tag{4.16}$$

$$\chi^q_2(\vec{\omega}) = \beta\xi \sum_{i,j} C_{ij}(\vec{\omega})\, \frac{\partial}{\partial \kappa_i} \frac{\partial}{\partial p_j}\, \Omega^{\lambda_g}_q(\alpha, \vec{\omega}; \beta, \vec{\kappa}; \xi, \vec{p})$$
$$+ \beta'\xi' \sum_{i,j} C_{ij}((1-\alpha)\vec{\omega})\, \frac{\partial}{\partial \kappa'_i} \frac{\partial}{\partial p'_j}\, \Omega^{\lambda_g}_q(\alpha, \vec{\omega}; \beta', \vec{\kappa}\,'; \xi', \vec{p}\,')\,, \tag{4.17}$$

$$\chi_3^q(\vec{R},\vec{\omega}) \;=\; 2\beta\xi \sum_{i,j} C_{ij}(\vec{R}-(1-\alpha)\vec{\omega})\,\frac{\partial}{\partial\kappa_i}\frac{\partial}{\partial p_j}\,\Omega_q^{\lambda_g}(\alpha,\vec{\omega};\beta,\vec{\kappa};\xi,\vec{p})\,, \tag{4.18}$$

$$\chi_4^q(\vec{R},\vec{\omega}) \;=\; 2\beta'\xi' \sum_{i,j} C_{ij}(\vec{R}-(1-\alpha)\vec{\omega})\,\frac{\partial}{\partial\kappa_i'}\frac{\partial}{\partial p_j'}\,\Omega_q^{\lambda_g}(\alpha,\vec{\omega};\beta',\vec{\kappa}\,';\xi',\vec{p}\,')\,, \tag{4.19}$$

and similarly for diffractive gluon excitations. Notice that the resulting cross section depends on the hard scale $r_{\rm hard}\sim 1/M_h$ (or $1/m_Q$) as $\sigma(pp\to Q\bar{Q}h+X)\propto r_{\rm hard}^4$, which implies that the diffractive Higgsstrahlung process under consideration is of higher twist nature.

For the sake of convenience, we further modify the phase space integrals in Eq. (4.7) by introducing new variables $\vec{r}_2\to\vec{r}_{12}$ and $\vec{r}_3\to\vec{r}_{13}$, so that,

$$\int d^2r_1d^2r_2d^2r_3\,e^{-a(r_1^2+r_2^2+r_3^2)}\delta(\vec{r}_1+\vec{r}_2+\vec{r}_3)=\frac{1}{9}\int d^2r_{12}d^2r_{13}e^{-\frac{2a}{3}(r_{12}^2+r_{13}^2+\vec{r}_{12}\vec{r}_{13})}\,. \tag{4.20}$$

Integration over $\vec{r}_{12}$ and $\vec{r}_{13}$ with appropriate weight factors proportional to C_{ij}, can also be taken analytically, giving rise to rather lengthy expressions. The remaining phase space integrals in Eq. (4.7) can be taken only numerically.

As long as the forward diffractive cross section, Eq. (4.7), is known, the total single diffractive cross section can be evaluated as

$$\frac{d\sigma_{sd}}{d\Omega_{\rm diff}}\simeq\frac{1}{B_{\rm sd}(s)}\,\frac{d\sigma_{sd}}{d\Omega_{\rm diff}\,d|t|}\Big|_{t\to 0} \tag{4.21}$$

where $d\Omega_{\rm diff}$ is the element of the phase space volume associated with the diffractive system $X+Q\bar{Q}+h$; $t=-|\delta_\perp|^2$ is the t-channel momentum transfer squared; and $B_{sd}(s)\simeq\langle r_{ch}^2\rangle_p/3+2\alpha'_{I\!P}\ln(s/s_0)$ is the t-slope of the of the differential single diffractive cross section, which is expected to be similar to the t-slope measured in diffractive DIS.

V. LOOP-INDUCED SINGLE DIFFRACTIVE HIGGS BOSON PRODUCTION

In this work, we discuss the loop-induced $gg\to h$ subprocess for the purposes of comparison with the tree-level Higgsstrahlung $gg\to h+(Q\bar{Q})$ subprocess off heavy $Q=c,b,t$ quarks at forward rapidities with a single-diffractive topology. In this first calculation, we perform the analysis of observables in the leading order in QCD virtual corrections while a dominant part from the QCD soft-gluon resummation expected to be effectively accounted for by the virtue of the dipole formulation used in this work as discussed in e.g. Refs. [24, 25, 27, 37, 38]).

In a realistic case of relatively small gluon transverse momenta (and hence virtualities) compared to the Higgs boson mass, $|\vec{q}|,\,|\vec{q}\,'|\ll M_h$, the amplitude of the on-shell loop-induced gg-fusion process $g(q)g(q')\to h(p)$ is given by the well-known expression (see e.g. Refs. [5, 8, 13, 39]),

$$T^f_{\mu\nu}(q,q')\simeq i\frac{\sqrt{\alpha_s}}{2\pi}\frac{1}{v}\big[(qq')g_{\mu\nu}-q_\mu q'_\nu\big]\,G_1^f\Big(\frac{M_h^2+i\epsilon}{4m_f^2}\Big)\,, \tag{5.1}$$

where $f=c,b,t$ are the heavy quark flavors in the loop. As was shown in Ref. [40], the gluon virtualities contribute not more than a fraction of percent in the kinematics of interest and thus are neglected here. The form factor G_1^f is the standard one and can be found in the

above references. For a color singlet state production the color factor will be absorbed into the dipole cross section. Normalization in Eq. (5.1) accounts for the fact that $\sqrt{\alpha_s}$ factor has been included into the quark-target scattering amplitude.

While in this first calculation of the single diffractive Higgs boson production in the dipole approach we use the leading order $gg \to h$ hard matrix element (5.1), one could potentially extend this analysis and include virtual QCD corrections in a similar way as was done in inclusive Higgs boson production. For this purpose one would need to multiply the leading-order cross section by a next-to-leading order $K_{\rm NLO} \simeq 1.5$ factor which is almost independent on the Higgs mass [8].

For our purposes here, consider pp scattering with a Higgs boson produced in the forward direction (zero momentum transfer to the target proton) via the gg fusion mechanism due to a quark and gluon excitations, respectively. The transverse momenta of the Higgs boson and final quark are given by,

$$\vec{p} = \vec{q} + \vec{q}' = -\vec{\pi} + \alpha\vec{q}, \qquad \vec{p}_2 = -\vec{q}' = \vec{\pi} + (1-\alpha)\vec{q},$$

respectively. Using the gluon polarization tensor in the form,

$$\sum_\lambda \epsilon^\mu_\lambda \epsilon^{*\,\nu}_\lambda = \frac{k^\mu_\perp k^\nu_\perp}{|\vec{k}\,|^2}\,, \qquad k^\mu_\perp = (0,\,\vec{k},\,0)\,,$$

one obtains the following normalized projection of the amplitude implicitly summed over the gluon polarisations

$$A^f_{g^*g^*\to h} \equiv T^f_{\mu\nu}\frac{q^\mu_\perp q'^\nu_\perp}{|\vec{q}||\vec{q}'|} \simeq -i\frac{\sqrt{\alpha_s}}{4\pi}\frac{M_h^2}{v}\,G_1^f\Big(\frac{M_h^2+i\epsilon}{4m_f^2}\Big)\,, \tag{5.2}$$

where $\vec{q}' \simeq -\vec{q}$, $p \equiv |\vec{p}\,|$, and we consider moderate values of the Higgs transverse momentum $m_q \ll p \lesssim M_h$. Up to a dimensionless normalization factor, the amplitude of Higgs boson production in quark-proton scattering acquires the form,

$$M^{q,g}_\triangle(\alpha,\vec{p}_2;\vec{q}) \sim \Psi^{q,g}_\triangle(\alpha,\vec{p}_2)\,\mathcal{V}(\vec{q})\,, \quad \Psi^{q,g}_\triangle(\alpha,\vec{p}_2) = \frac{\Gamma_{q,g}(\alpha,\vec{p}_2)}{2M_h\,D_3(\alpha,\vec{p}_2)}\sum_{f=c,b,t} A^f_{g^*g^*\to h}\,, \tag{5.3}$$

where $\mathcal{V}(\vec{q})$ is the quark-target scattering amplitude. The amplitude Γ_q for gluon emission off a projectile quark q reads,

$$\Gamma_q(\alpha,\vec{\pi}) \;=\; \frac{\sqrt{\alpha_s(|\vec{\pi}|)}}{|\vec{\pi}|}\,\chi^\dagger\Big\{(2-\alpha)|\vec{\pi}|^2 + i\alpha^2 m_q\,[\vec{\sigma}\times\vec{\pi}]\cdot\vec{n}\Big\}\chi\,, \tag{5.4}$$

which corresponds to $\Gamma^\lambda_q(\alpha,\vec{\pi})$ defined in Eqs. (2.18) and (2.20) with the transverse polarisation vector of the hard gluon $\vec{\epsilon}_\lambda(\vec{\pi}) = \vec{\pi}/|\vec{\pi}|$. The corresponding contribution from the diffractive excitation of gluons should be included via the $g \to gg^*$ splitting amplitude

$$\Gamma_g(\alpha,\vec{\pi}) = 2\sqrt{\alpha_s(|\vec{\pi}|)}\,(1-\alpha)(\vec{e}_f\cdot\vec{e}_{in})|\vec{\pi}|\,, \tag{5.5}$$

and one should take into account the difference in the overall color factor between (anti)quark and gluon diffractive excitations,

$$\rho_q(x) + \rho_{\bar{q}}(x) \;\to\; \left(\frac{9}{4}\right)^2 g(x)\,. \tag{5.6}$$

Notice that in the limits of either small fractional momentum $x \ll 1$, or/and large, $\alpha \to 1$, corresponding to the forward Higgs boson production, the contribution from the diffractive gluon excitation naturally vanishes.

In the case of diffraction, the second "color screening" gluon couples to the same valence quark before and after the emission vertex of the hard gluon in order to compensate the large virtuality, giving rise to the dipole cross section. Converting the amplitudes into impact parameter space,

$$\Phi_{\triangle}(\alpha,\vec{\omega}) = \int \frac{d^2\vec{\pi}}{(2\pi)^2}\, e^{-i\vec{\pi}\cdot\vec{\omega}}\, \Psi_{\triangle}(\alpha,\vec{\pi})\,, \qquad V(\vec{b}) = \int \frac{d^2\vec{q}}{(2\pi)^2}\, e^{-i\vec{q}\cdot\vec{b}}\, \mathcal{V}(\vec{q})\,, \tag{5.7}$$

the amplitude of single diffractive Higgs production in quark-proton scattering takes the following form,

$$M^D_{\triangle}(\vec{\pi},\vec{q}) \;=\; \int d^2\vec{b}\, d^2\vec{\omega}\, e^{i\vec{q}\cdot\vec{b}+i\vec{\pi}\cdot\vec{\omega}}\, \Phi_{\triangle}(\vec{\omega}) \Big[\mathrm{Im}\, f_{el}(\vec{b},\vec{\omega}) - \mathrm{Im}\, f_{el}(\vec{b},(1-\alpha)\vec{\omega})\Big]\,.$$

Eventually, after integration over all d.o.f. in the proton wave function, except the active quark momentum, the diffractive cross section at the hadronic level for (anti)quark excitations can be written as follows,

$$\begin{aligned}\frac{d\sigma_q(pp\to phX)}{d^2\vec{p}\, d\ln\alpha\, d^2\vec{\delta}_\perp}\Big|_{\delta_\perp\to 0} &= \frac{1}{(2\pi)^2}\frac{1}{64\pi^2}\sum_q \int d^2\vec{\omega} d^2\vec{\omega}\,'\, dx_q \Big[\rho_q(x_q)+\rho_{\bar q}(x_q)\Big] \\ &\times \Phi^q_{\triangle}(\alpha,\vec{\omega})\Phi^{q*}_{\triangle}(\alpha,\vec{\omega}\,')\,\Sigma_{\triangle}(\alpha,\vec{\omega})\Sigma_{\triangle}(\alpha,\vec{\omega}\,')\, e^{i\vec{p}\cdot(\vec{\omega}-\vec{\omega}\,')}\,,\end{aligned} \tag{5.8}$$

and similarly for the gluon excitations. Here, $\vec{p} \simeq -\vec{\pi}$ in the limit of forward scattering, and

$$\Sigma_{\triangle} = \frac{3}{2}\Big[\sigma(\vec{\omega}) - \sigma\big((1-\alpha)\vec{\omega}\big)\Big]\,,$$

is the effective dipole amplitude, where the factor 3 accounts for valence quark permutations. In the case of a large Higgs boson transverse momentum, $|\vec{p}| \gg m_q$, we have $\omega \ll r_{ij} \sim R$, so that the effective dipole amplitude to the leading order acquires the simple form,

$$\Sigma_{\triangle} \simeq \frac{3\sigma_0}{2R_0^2}\,\alpha(2-\alpha)\omega^2$$

where $\sigma_0 = \sigma_0(x)$, $R_0 = R_0(x)$ are x-dependent in this case, and are defined according to the GBW parameterization [26]. This makes possible to perform almost all integrations in Eq. (5.8) analytically. For example, the integration over $\vec{p}$ in Ref. (5.8) leads to,

$$\begin{aligned}\frac{d\sigma_q(pp\to phX)}{d\ln\alpha} &= \frac{9\sigma_0^2}{256\, B_{\rm sd}(s)}\,\frac{\alpha^2(2-\alpha)^2}{R_0^4} \\ &\times \sum_q \int dx_q \Big[\rho_q(x_q)+\rho_{\bar q}(x_q)\Big] \int_0^{\omega_{\rm cut}} d\omega^2\, \omega^4\, |\Phi^q_{\triangle}(\alpha,\vec{\omega})|^2\,,\end{aligned} \tag{5.9}$$

where $\omega_{\rm cut} \simeq 1/p_{\rm cut}$ is related to the bottom bound for the Higgs transverse momentum $p_{\rm cut}$, which is related to the detector limitations. The function $\Phi^q_{\triangle}$ in the integrant in (5.9) can

be represented as,

$$|\Phi^q_{\triangle}(\alpha,\vec{\omega})|^2 \;=\; \frac{\alpha_s(\omega^{-1})}{4M_h^2}\,\frac{m_q^2\alpha^2}{32}\Big[4(2-\alpha)^2\big(I_0(m_q\alpha\omega)-L_0(m_q\alpha\omega)\big)^2 \qquad (5.10)$$
$$+\;\frac{\alpha^2}{\pi^2}\big(2-2\pi I_1(m_q\alpha\omega)+\pi L_{-1}(m_q\alpha\omega)+\pi L_1(m_q\alpha\omega)\big)^2\Big]\,|A^{top}_{g^*g^*\to h}|^2,$$

in terms of the modified Bessel function of the first kind $I_n(x)$ and the modified Struve function $L_n(x)$.

Alternatively, in order to obtain the dependence on Higgs transverse momentum p, one could integrate over $\vec{\omega}$ to arrive at a different expression,

$$\frac{d\sigma_q(pp\to phX)}{dp^2\,d\ln\alpha}=\frac{9\sigma_0^2}{256\,B_{\rm sd}(s)}\,\frac{\alpha^2(2-\alpha)^2}{R_0^4(2\pi)^2}\,|\Xi^q_{\triangle}(\alpha,\vec{p})|^2\sum_q\int dx_q\Big[\rho_q(x_q)+\rho_{\bar q}(x_q)\Big],$$

or at the differential distribution in Higgs fractional momentum, $x_1\simeq(M_h/\sqrt{s})\,e^{+Y_h}$, $Y_h>0$, which in the forward limit has the form,

$$\frac{d\sigma_q(pp\to phX)}{dp^2\,dx_1}=\frac{9\sigma_0^2}{256\,B_{\rm sd}(s)}\frac{1}{R_0^4(2\pi)^2}\sum_q\int_{x_1}^1 d\alpha\Big[\rho_q\Big(\frac{x_1}{\alpha}\Big)+\rho_{\bar q}\Big(\frac{x_1}{\alpha}\Big)\Big](2-\alpha)^2|\Xi^q_{\triangle}(\alpha,\vec{p})|^2.$$

Here, to a good approximation,

$$\Xi^q_{\triangle}(\alpha,\vec{p})=\int d^2\vec{\omega}\,\omega^2\,\Phi^q_{\triangle}(\alpha,\vec{\omega})\,e^{i\vec{p}\cdot\vec{\omega}}=-\sum_i\frac{\partial}{\partial p_i}\frac{\partial}{\partial p^i}\Psi^q_{\triangle}(\alpha,\vec{p}\,),$$
$$|\Xi^q_{\triangle}(\alpha,\vec{p})|^2\simeq\frac{\alpha_s(p)}{4M_h^2}\,\frac{18\alpha^4m_q^2}{p^8}\,|A^{top}_{g^*g^*\to h}|^2\,, \qquad (5.11)$$

where $p\gg m_q$ and only the dominant top quark contribution $A^{top}_{g^*g^*\to h}$ defined in Eq. (5.2), is kept. From the last formula we see that the Higgs boson transverse momentum dependence is particularly strong and sharply peaked at low p. Note that the corresponding total cross section effectively behaves as a hard scale $r_{\rm hard}\sim 1/M_h$ to the fourth power in the case of valence/sea quark excitations, i.e. $\sigma_q(pp\to phX)\propto r^4_{\rm hard}$. The single diffractive Higgs production occured via diffractive excitation of a projectile (anti)quark, which is a higher twist effect and thus is stronger suppressed than the leading-twist diffractive Drell-Yan process [21, 22], where $\sigma(pp\to p\gamma^*X)\propto r^2_{\rm hard}$. The strong $r_{\rm hard}$ dependence of the diffractive quark excitation might signal about importance of the higher order terms, extending beyond the two-gluon exchange approximation.

In the case of diffractive gluon excitation, Eq. (5.11) gets the following form,

$$|\Xi^g_{\triangle}(\alpha,\vec{p})|^2\simeq\frac{\alpha_s(p)}{4M_h^2}\,\frac{8(1-\alpha)^2}{p^6}\,|A^{\rm top}_{g^*g^*\to h}|^2\,, \qquad (5.12)$$

so it is a leading twist, and the corresponding contribution to the total cross section behaves as $\sigma_g(pp\to phX)\propto r^2_{\rm hard}$ but is on the other hand suppressed in the forward region $\alpha\to 1$. Now we turn to a discussion of numerical results.

VI. NUMERICAL RESULTS

Consider now the general properties of differential observables corresponding to the inclusive and single diffractive Higgsstrahlung and the loop-induced Higgs boson production processes. To start with, the inclusive gluon-generated h and $Q\bar{Q}h$ production cross sections are shown in Fig. 4 as functions of the Higgs boson transverse momentum p, $d\sigma_{incl}/dp^2$ (left), and heavy (anti)quark momentum κ, $d\sigma_{incl}/d\kappa^2$ (right). The $gg \to t\bar{t} + h$ and $gg \to b\bar{b} + h$ cross sections have the same order of magnitude values for intermediate Higgs transverse momenta $\sim 50 - 100$ GeV since the amplitudes squared behave with the hard scales (which are the transverse heavy quark mass $M_{Q\perp}$ and the Higgs mass $M_{H\perp}$) very roughly as

$$|A|^2 \sim \frac{g^2_{HQQ}}{M^2_{Q\perp}\, M^2_{H\perp}}\,, \tag{6.1}$$

such that the quark mass dependence in the Yukawa coupling squared $g^2_{HQQ} \sim M^2_Q$ is largely eliminated. Also, the top contribution appears to be flatter than that for the bottom components and starts decreasing at much larger transverse momenta then the bottom one. The numerical results are found to be in a good overall agreement with those in Refs. [13, 15]. Note, here and below the contribution of longitudinally polarized gluons to the integrated cross section does not exceed few percents and can be safely neglected.

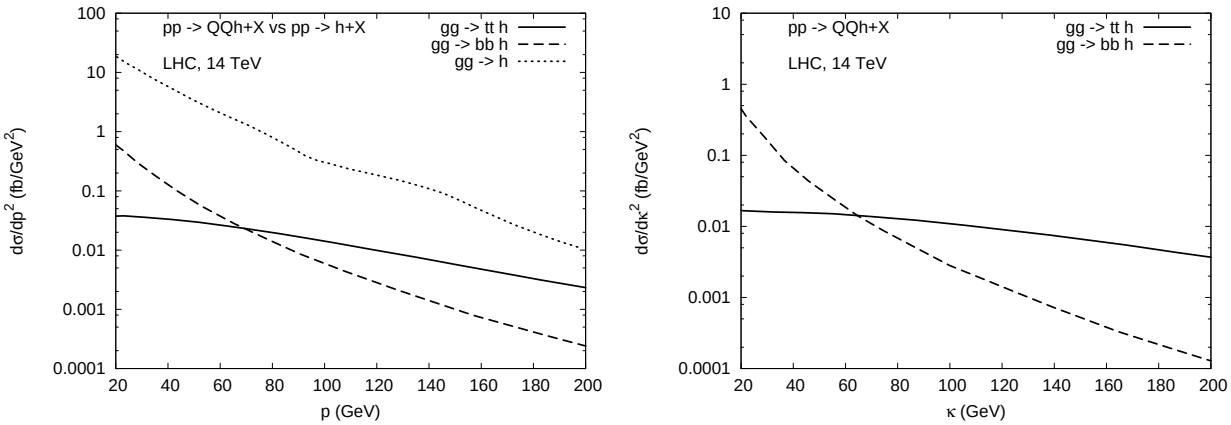

FIG. 4: Differential cross sections for inclusive Higgsstrahlung off $t\bar{t}$ (solid lines) and $b\bar{b}$ (dashed lines) pairs, as well as for the inclusive loop-induced Higgs production (dotted line), as functions of Higgs boson transverse momentum p (left panel), while the corresponding inclusive Higgsstrahlung cross sections differential in heavy (anti)quark transverse momentum κ are shown in the right panel. The Higgstrahlung components predominantly come from the sea/valence quark excitations. The pp c.m.s. energy here and below is $\sqrt{s} = 14$ TeV.

Let us consider the corresponding diffractive components. The loop-induced single diffractive Higgs production, $pp \to h + X + p$, was calculated above, Eq. (5.11), within the dipole formalism. In Fig. 5 we show the differential cross sections $d\sigma/dp^2$ and $d\sigma/dx_1$ vs Higgs boson transverse momentum $p \equiv |\vec{p}|$ (left) and longitudinal momentum fraction $x_1 \gg x_2$ (right), respectively. The latter are compared with corresponding diffractive Higgsstrahlung components. We imposed the realistic ATLAS detector constraints [17–19] on forward Higgs boson rapidity $0 < Y_h < 2.5$, and the cuts on Feynman x_F associated with the recoil target

proton, $0.8 < x_F < 0.998$. The contributions of diffractive valence/sea (anti)quark excitations relevant in the region of large $x_1 \to 1$ are shown here. A proper relation of the experimental acceptances for decay products with actual phase space bounds on producing Higgs boson and heavy quarks is the matter of a dedicated Monte-Carlo detector-level simulation, which we do not aim at in this first calculation of diffractive Higgsstrahlung.

The differential cross sections for the diffractive Higgsstrahlung process associated with top (solid lines) and bottom (dashed lines) quark pair production as functions of the Higgs transverse momentum p and longitudinal fraction x_1, as well as heavy (anti)quark transverse momentum κ, are presented in Figs. 5 and 6, respectively. In these plots, only the dominating diffraction sea/valence quark excitations contribution is shown. In the forward region $x_1 \gtrsim 0.5$ the loop-induced contribution $gg \to h$ dominates over the Higgsstrahlung components $gg \to t\bar{t}h$ and $gg \to b\bar{b}h$, as well as at very small Higgs boson transverse momenta. The top quark contribution to the Higgsstrahlung part is typically small except the central rapidity regions where it is, however, restricted by kinematics. The bottom contribution can be as important as the top one at low Higgs transverse momenta p, while at large $p > 60$ GeV the top component becomes strongly dominating over the others (charm contribution, suppressed by a few orders of magnitude, is not shown). Both contributions, especially the top one, expose somewhat steeper x_1-dependence than that for the loop-induced Higgs boson production. Also, similarly to the inclusive case the top quark component appears to be much flatter compared to the bottom one due to reasons outlined above and becomes rather strongly dominating for large Higgs boson transverse momenta. The actual effective dipole amplitudes, wave functions and the phase space treatment are very much more complicated in the diffractive case, such that a quantitative difference emerges as a somewhat stronger top domination over the bottom for diffraction than that for the inclusive case (see above).

We conclude that the main part of the single diffractive Higgs boson production cross section at large Higgs boson transverse momenta comes from the $t\bar{t}h$ Higgsstrahlung component. The contribution of diffractive gluon excitations to the Higgsstraglung processes is vanishingly small there, similarly to the loop-induced Higgs boson production. This happens because the cross section of hard excitation of a transversely polarized gluon behaves

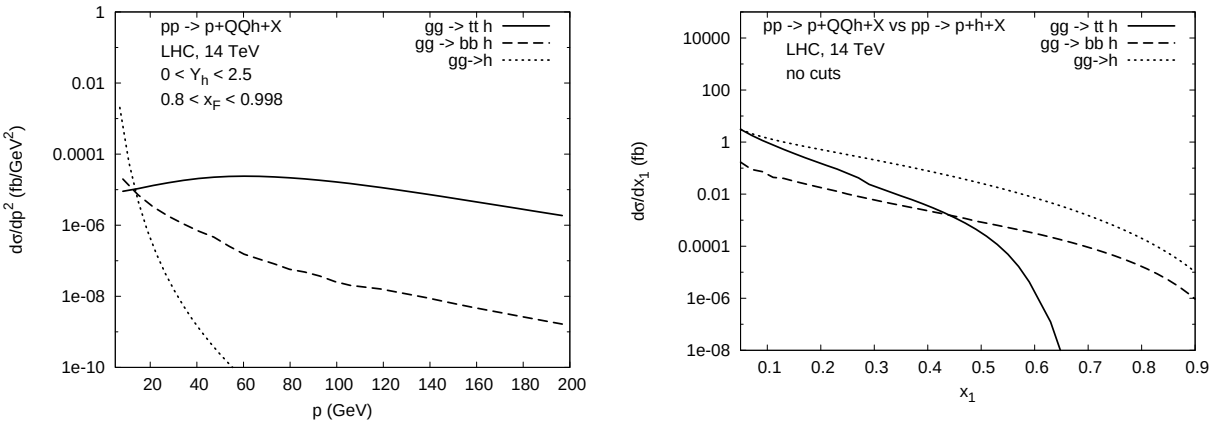

FIG. 5: Differential cross sections for diffractive Higgsstrahlung off $t\bar{t}$ (solid lines) and $b\bar{b}$ (dashed lines) pairs vs loop-induced production cross section (dotted lines) as function of Higgs boson transverse momentum p (left) and longitudinal momentum fraction x_1 (right). The ATLAS kinematic constraints on rapidities of Q, $\bar{Q}$ and h and Feynman variable x_F are imposed in the left plot.

as $\propto (1-\alpha)^2$ and is suppressed at forward rapidities.

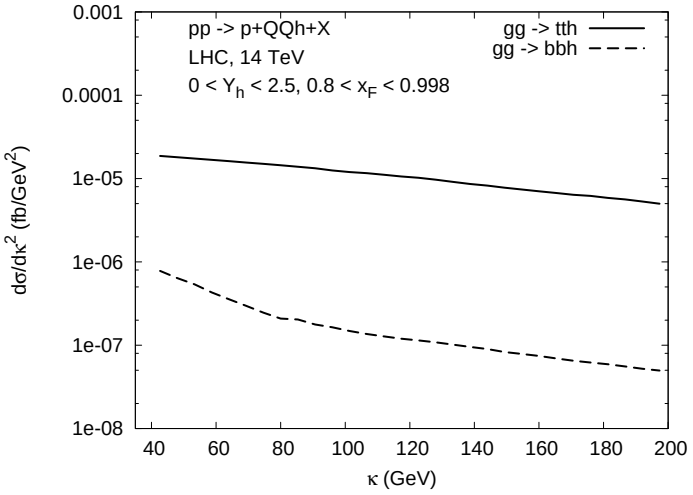

FIG. 6: Differential cross sections of single-diffractive Higgsstrahlung off $t\bar{t}$ (solid lines) and $b\bar{b}$ (dashed lines) pairs as function of transverse momentum κ of the heavy (anti)quark. The ATLAS kinematical constraints on the rapidities of Q, $\bar{Q}$ and h and Feynman variable x_F are imposed.

VII. CONCLUSION

Here we presented the first evaluation of the single diffractive Higgsstrahlung process off heavy (top and bottom) quarks and the diffractive loop-induced Higgs boson production performed within the light-cone dipole approach.

We derived analytic formulae for diffractive amplitudes and numerically evaluated the corresponding differential cross sections, $d\sigma/dp^2$, $d\sigma/d\kappa^2$ and $d\sigma/dx_1$, as functions of transverse momenta of Higgs (p) and final-state heavy quark (κ), and the fractional momentum of the Higgs boson (x_1), respectively. The dominant contribution to the diffractive $t\bar{t}+h$ and $b\bar{b}+h$ production at forward rapidities comes from the diffractive excitation of the incoming valence/sea (anti)quarks, similarly to the loop-induced Higgs boson production. Even though, the production of a Higgs boson h associated with a top quark $t\bar{t}$ pair is found to be of the higher twist, it has the largest cross section at large Higgs transverse momentum $p > 60$ GeV, so can be considered as the major Higgs boson production channel at forward and mid-rapidities.

As an outlook for the future studies, there is an open question about characteristics of the background to the diffractive Higgsstrahlung process, which would be the next step. Naively, one could expect that the major part of the QCD/EW backgrounds comes from the multiparton interactions, which gives rise to $(t\bar{t})+(b\bar{b})$ system production (with invariant mass of $b\bar{b}$ pair around the Higgs boson resonance), e.g. from two consequent hard gg-fusion subprocesses. These, however, are expected to be strongly suppressed in the diffractive case by both kinematical constraints, Higgs resonance requirement and by extra powers of QCD couplings (compared with the large Higgs-top Yukawa coupling in the Higgsstrahlung case). Tagging on both top and bottom quarks at forward rapidities, accompanied by the large rapidity gap requirement, would certainly help in increasing the signal-to-background

ratio, which is expected to be higher than for diffractive loop-induced Higgs production, which involves no heavy quark production, or other distinct signatures to trigger on (while $b\bar{b}$ backgrounds are typically abundant, see e.g. Ref. [41]). Nevertheless, a more detailed investigation of the QCD backgrounds would certainly be required for the proof of this concept.

Acknowledgments

Useful discussions with Valery Khoze, Antoni Szczurek and Gunnar Ingelman are gratefully acknowledged. This study was partially supported by Fondecyt (Chile) grants 1120920, 1130543 and 1130549, and by ECOS-Conicyt grant No. C12E04.

---

[1] G. Aad *et al.* [ATLAS Collaboration], Phys. Lett. B **716**, 1 (2012) [arXiv:1207.7214 [hep-ex]]; Science **338**, 1576 (2012).

[2] S. Chatrchyan *et al.* [CMS Collaboration], Phys. Lett. B **716**, 30 (2012) [arXiv:1207.7235 [hep-ex]];
Science **338**, 1569 (2012).

[3] M. S. Carena and H. E. Haber, Prog. Part. Nucl. Phys. **50**, 63 (2003) [hep-ph/0208209].

[4] S. Dittmaier *et al.* [LHC Higgs Cross Section Working Group Collaboration], arXiv:1101.0593 [hep-ph]; arXiv:1201.3084 [hep-ph];
S. Heinemeyer *et al.*, arXiv:1307.1347 [hep-ph].

[5] H. M. Georgi, S. L. Glashow, M. E. Machacek and D. V. Nanopoulos, Phys. Rev. Lett. **40**, 692 (1978).

[6] A. Djouadi, M. Spira and P. M. Zerwas, Phys. Lett. B **264**, 440 (1991).

[7] S. Dawson, Nucl. Phys. B **359**, 283 (1991).

[8] M. Spira, A. Djouadi, D. Graudenz and P. M. Zerwas, Nucl. Phys. B **453**, 17 (1995) [hep-ph/9504378].

[9] C. Anastasiou and K. Melnikov, Nucl. Phys. B **646**, 220 (2002) [hep-ph/0207004].

[10] V. Ravindran, J. Smith and W. L. van Neerven, Nucl. Phys. B **665**, 325 (2003) [hep-ph/0302135].

[11] S. Catani, D. de Florian, M. Grazzini and P. Nason, JHEP **0307**, 028 (2003) [hep-ph/0306211].

[12] S. Actis, G. Passarino, C. Sturm and S. Uccirati, Phys. Lett. B **670**, 12 (2008) [arXiv:0809.1301 [hep-ph]].

[13] A. V. Lipatov and N. P. Zotov, Eur. Phys. J. C **44**, 559 (2005) [hep-ph/0501172].

[14] A. V. Lipatov, M. A. Malyshev and N. P. Zotov, arXiv:1402.6481 [hep-ph].

[15] A. V. Lipatov and N. P. Zotov, Phys. Rev. D **80**, 013006 (2009) [arXiv:0905.1894 [hep-ph]].

[16] V. A. Khoze, A. D. Martin and M. G. Ryskin, Phys. Lett. **B401** (1997) 330; Eur. Phys. J. **C14** (2000) 525; Eur. Phys. J. **C19** (2001) 477 [Erratum-ibid. **C20** (2001) 599]; Eur. Phys. J. **C23** (2002) 311;
A. B. Kaidalov, V. A. Khoze, A. D. Martin and M. G. Ryskin, Eur. Phys. J. **C33** (2004) 261.

[17] S. Heinemeyer, V. A. Khoze, M. G. Ryskin, W. J. Stirling, M. Tasevsky and G. Weiglein, Eur. Phys. J. C **53**, 231 (2008) [arXiv:0708.3052 [hep-ph]].

[18] S. Heinemeyer, V. A. Khoze, M. G. Ryskin, M. Tasevsky and G. Weiglein, Eur. Phys. J. C **71**, 1649 (2011) [arXiv:1012.5007 [hep-ph]].

[19] M. Tasevsky, Eur. Phys. J. C **73**, 2672 (2013) [arXiv:1309.7772 [hep-ph]].

[20] B. Z. Kopeliovich, L. I. Lapidus and A. B. Zamolodchikov, JETP Lett. **33**, 595 (1981) [Pisma

Zh. Eksp. Teor. Fiz. **33**, 612 (1981)].
[21] B. Z. Kopeliovich, I. K. Potashnikova, I. Schmidt and A. V. Tarasov, Phys. Rev. D **74**, 114024 (2006) [hep-ph/0605157].
[22] R. S. Pasechnik and B. Z. Kopeliovich, Eur. Phys. J. C **71**, 1827 (2011) [arXiv:1109.6695 [hep-ph]].
[23] R. Pasechnik, B. Kopeliovich and I. Potashnikova, Phys. Rev. D **86**, 114039 (2012) [arXiv:1204.6477 [hep-ph]].
[24] B. Z. Kopeliovich, I. K. Potashnikova, I. Schmidt and A. V. Tarasov, Phys. Rev. D **76**, 034019 (2007) [hep-ph/0702106 [HEP-PH]].
[25] B. Z. Kopeliovich, A. Schäfer and A. V. Tarasov, Phys. Rev. **D62**, 054022 (2000) [arXiv:hep-ph/9908245].
[26] K. J. Golec-Biernat, M. Wusthoff, Phys. Rev. **D59**, 014017 (1998). [hep-ph/9807513].
[27] S. J. Brodsky, A. S. Goldhaber, B. Z. Kopeliovich and I. Schmidt, Nucl. Phys. B **807**, 334 (2009) [arXiv:0707.4658 [hep-ph]].
[28] S. J. Brodsky, B. Kopeliovich, I. Schmidt and J. Soffer, Phys. Rev. D **73**, 113005 (2006) [hep-ph/0603238].
[29] J. F. Gunion and G. Bertsch, Phys. Rev. D **25**, 746 (1982).
[30] B. Z. Kopeliovich, A. V. Tarasov and A. Schafer, Phys. Rev. C **59**, 1609 (1999) [hep-ph/9808378].
[31] B. Z. Kopeliovich, I. K. Potashnikova, B. Povh and I. Schmidt, Phys. Rev. D **76**, 094020 (2007).
[32] B. Z. Kopeliovich, H. J. Pirner, A. H. Rezaeian and I. Schmidt, Phys. Rev. D **77**, 034011 (2008) [arXiv:0711.3010 [hep-ph]].
[33] B. Z. Kopeliovich, I. K. Potashnikova, I. Schmidt and J. Soffer, Phys. Rev. D **78**, 014031 (2008) [arXiv:0805.4534 [hep-ph]].
[34] B. Z. Kopeliovich, A. H. Rezaeian, I. Schmidt, Phys. Rev. **D78**, 114009 (2008) [arXiv:0809.4327 [hep-ph]].
[35] R. M. Barnett *et al.*, Rev. Mod. Phys. 68, 611 (1996).
[36] S. Amendolia *et al.*, Nucl. Phys. **B277**, 186 (1986).
[37] J. Raufeisen, J. -C. Peng and G. C. Nayak, Phys. Rev. D **66**, 034024 (2002) [hep-ph/0204095].
[38] B. Z. Kopeliovich and J. Raufeisen, Lect. Notes Phys. **647**, 305 (2004) [hep-ph/0305094].
[39] D. Graudenz, M. Spira and P. M. Zerwas, Phys. Rev. Lett. **70**, 1372 (1993).
[40] R. S. Pasechnik, O. V. Teryaev and A. Szczurek, Eur. Phys. J. C **47**, 429 (2006) [hep-ph/0603258].
[41] R. Maciula, R. Pasechnik and A. Szczurek, Phys. Rev. D **83**, 114034 (2011) [arXiv:1011.5842 [hep-ph]].